Reactive organic species in the northern extratropical lowermost stratosphere: Seasonal variability and implications for OH

H. A. Scheeren,[1,2] H. Fischer,[2] J. Lelieveld,[2] P. Hoor,[2,7] J. Rudolph,[4] F. Arnold,[5] B. Bregman,[3] C. Brühl,[2] A. Engel,[6] C. van der Veen,[1] and D. Brunner[7]

[1]   We present $C_2 - C_6$ nonmethane hydrocarbon (NMHC) measurements from canister samples obtained in the extratropical lower stratosphere during the fall (November/December 1995), winter (March 1997), and summer seasons (July 1998) as part of the stratosphere-troposphere experiments by aircraft measurements campaign. The flights were carried out from Amsterdam (Netherlands, 52°N, 4.5°E) during fall, from Kiruna (Sweden, 68°N, 20°E) during winter, and from Timmins (Canada, 48.2°N, 70.3°W) during summer. The NMHC measurements have been evaluated along with concurrent in situ measurements of acetone (CH_3COCH_3), CO, O_3, N_2O, and CFC-12 (CCl_2F_2). The vertical distributions of NMHC and acetone as a function of O_3 and potential temperature in the lowermost stratosphere show a strong seasonality. Enhanced concentrations of NMHC + CH_3COCH_3 were found during July up to potential temperatures of $\Theta = 370$ K, whereas during March this was limited to $\Theta = 340$ K, in agreement with stronger isentropic cross-tropopause transport during summer. Increasing methyl chloride (CH_3Cl) concentrations with altitude were measured during July, pointing to mixing at the subtropical tropopause. During summer and fall, mean NMHC + acetone concentrations were more than a factor of 2 higher than that during winter. Box model calculations indicate that the observed acetone levels of 0.5–1 ppbv can explain 30–50% of the enhanced OH radical concentrations in the summertime lowermost stratosphere. Using mass balance calculations, we show that a significant tropospheric fraction ($\leq 30\%$) was present up to $\Theta = 370$ K in the summertime lowermost stratosphere. During winter, the tropospheric fraction approached zero at about $\Theta = 350$ K. The time between selected troposphere-to-stratosphere mixing events and the aircraft measurements has been estimated at 3–14 days. Our results emphasize that isentropic cross-tropopause transport can be a fast process occurring on timescales of days to weeks.   *INDEX TERMS:* 0340 Atmospheric Composition and Structure: Middle atmosphere—composition and chemistry; 0341 Atmospheric Composition and Structure: Middle atmosphere—constituent transport and chemistry (3334); 3362 Meteorology and Atmospheric Dynamics: Stratosphere/troposphere interactions; *KEYWORDS:* airborne measurements, chemical composition, cross-tropopause transport

1. Introduction

[2]   In recent years there has been an increasing interest in the chemical composition of the extratropical lowermost stratosphere, located between the local tropopause and the 380-K potential temperature (Θ) isentrope, the latter coincident with the mean tropical tropopause [*Holton et al.*, 1995]. The lowermost stratosphere has thus been addressed in modeling studies [e.g., *Chen*, 1995; *Holton et al.*, 1995, and references therein; *Bregman et al.*, 2000; *Dethof et al.*, 2000; *Rood et al.*, 1997; *Wernli and Bourqui*, 2002] and measurement campaigns [e.g., *Bamber et al.*, 1984; *Kritz et al.*, 1991; *Poulida et al.*, 1996; *Appenzeller et al.*, 1996; *Bregman et al.*, 1997; *Lelieveld et al.*, 1997; *Singh et al.*, 1997; *Hintsa et al.*, 1998; *Flocke et al.*, 1999; *Ray et al.*, 1999; *Fischer et al.*, 2000; *Zahn*, 2001; *Hoor et al.*, 2002] to better understand and quantify cross-tropopause transport

[1]Institute for Marine and Atmospheric Research Utrecht (IMAU), Utrecht University, Utrecht, Netherlands.

[2]Max Planck Institute for Chemistry, Mainz, Germany.

[3]Royal Netherlands Meteorological Institute (KNMI), De Bilt, Netherlands.

[4]Centre for Atmospheric Chemistry, York University, North York, Ontario, Canada.

[5]Max Planck Institute for Nuclear Physics, Heidelberg, Germany.

[6]Institute for Meteorology and Geophysics, Johann Wolfgang Goethe University, Frankfurt, Germany.

[7]Institute for Atmospheric Science, Swiss Federal Institute of Technology, Zurich, Switzerland.

processes and their impact on the budget of ozone and other important trace gases. Bidirectional mass transfer across the tropopause can carry pollutants such as halocarbons, with a potential to destroy ozone, into the stratosphere, and on the other hand enrich the upper troposphere (UT) with ozone. Ozone near the tropopause acts as an effective greenhouse gas [*Lacis et al.*, 1990]. Hence understanding the ozone budget in the tropopause region is of great importance for climate change studies.

[3] The lowermost stratosphere can be considered as a distinct region where aged air masses descending from the stratosphere above, defined as "the overworld" ($\Theta \geq 380$ K) [*Hoskins*, 1991], mix with tropospheric air through several cross-tropopause transport processes [*Holton et al.*, 1995]. Diabatic descent brings aged stratospheric air from the overworld into the lowermost stratosphere, as first proposed by *Brewer* [1949], and is studied intensively thereafter both by experimental and modeling work [e.g., *Holton et al.*, 1995 and references therein; *Dessler et al.*, 1995; *Appenzeller et al.*, 1996; *Ray et al.*, 1999]. In addition, tropospheric air can enter the lowermost stratosphere adiabatically along isentropic surfaces crossing the subtropical or midlatitude tropopause. Isentropic cross-tropopause transport has been shown to occur from in situ measurements by *Kritz et al.* [1991], *Lelieveld et al.* [1997], *Hintsa et al.* [1998], *Vaughan and Timmins* [1998], *Fischer et al.* [2000], and *Zahn* [2001], and from modeling work by *Chen* [1995], *Dethof et al.* [2000], and *Seo and Bowman* [2001]. Finally, mixing can occur by diabatic ascent across isentropes at the extratropical tropopause associated with synoptic-scale disturbances (polar fronts) and deep convection in thunderstorms [e.g., *Fischer et al.*, 2003]. Since this process is believed to only affect the region near the tropopause [*Poulida et al.*, 1996; *Lelieveld et al.*, 1997], it can be assumed that isentropic transport is the main source of tropospheric air in the lowermost stratosphere.

[4] Transport from the troposphere to the stratosphere in the extratropics has a strong seasonal dependence, which results in a mixing layer above the local tropopause with a maximum depth in summer and a minimum during winter [e.g., *Chen*, 1995; *Dethof et al.*, 2000; *Hoor et al.*, 2002]. According to modeling work by *Chen* [1995] and *Dethof et al.* [2000] there is very little isentropic transport between $\Theta = 340$ and 360 K across the tropopause during winter due to the strong subtropical jet, which acts as a transport barrier. During the northern summer the subtropical jet is much weaker, allowing isentropic transport into the lowermost stratosphere driven by the Asian and Mexican monsoon circulations. Measurements by *Ray et al.* [1999] demonstrate that most of the air below $\Theta = 380$ K in the lowermost stratosphere during September has entered quasi-isentropically from the subtropical troposphere, whereas during May downward advection from the stratospheric overworld ($\Theta > 380$ K) was the dominant source of air. *Hoor et al.* [2002] identified a mixing layer in the lowermost stratosphere from correlations between CO and O_3 observed during the March 1997 and July 1998 stratosphere-troposphere experiments by aircraft measurement (STREAM) campaigns. They found a significant direct tropospheric influence up to $\Theta = 330$ K during March, while this mixing layer increased to $\Theta = 360$ K during July. This appeared to be caused by a stronger

contribution of subtropical tropospheric air mixed in at the subtropical jet.

[5] Thus far, most studies on the chemical composition and dynamics of the lowermost stratosphere have used relatively long-lived tracers (e.g., N_2O, CO_2, CH_4, SF_6, CFC-11 (CCl_3F), and CFC-12 (CCl_2F_2)) with lifetimes far exceeding typical exchange times between the lowermost stratosphere and upper troposphere, being on the order days to weeks [e.g., *Boering et al.*, 1994; *Lelieveld et al.*, 1997; *Dethof et al.*, 2000; *Andrews et al.*, 2001]. However, to our knowledge little attention has been given to the abundance of short-lived tracers such as nonmethane hydrocarbons [*Singh et al.*, 1997, 2000; *Flocke et al.*, 1999] and acetone in the lowermost stratosphere [*Arnold et al.*, 1997; *Wohlfrom et al.*, 1999; *Singh et al.*, 2000]. The occurrence and abundance of nonmethane hydrocarbons (NMHC) and acetone with relatively short photochemical lifetimes on the order of weeks can give insight into the frequency and timescales of mixing processes, which determine the tracer budgets in the lowermost stratosphere. Moreover, the stratospheric acetone budget is important because acetone photolysis is a source of peroxy and alkoxy radicals, which can enhance OH and HO_2 radical concentrations [*Singh et al.*, 1995].

[6] In this paper we focus on selected C_2-C_6 NMHC measurements from canister samples collected in the extratropical upper troposphere and lowermost stratosphere during November/December 1995, March 1997, and July 1998 as part of the STREAM project. In July 1998 methyl chloride (CH_3Cl) was measured as well. Methyl chloride forms the largest natural source of chlorine in the stratosphere, and its relative contribution is increasing due to the decline of man-made halocarbons. The NMHC data have been analyzed on the basis of concurrent in situ measurements of O_3, CO, acetone (CH_3COCH_3), N_2O, and CFC-12. The data have been applied to study the seasonality in the NMHC and acetone distributions in the lowermost stratospheric mixing layer. Furthermore, we present estimates of the fraction of tropospheric air transported into the mixing layer. We show results from a photochemical box model study, to investigate the role of observed acetone levels on OH formation in the lowermost stratosphere. Finally, we introduce a simple method to estimate the residence time of air masses in the lowermost stratosphere from elevated NMHC concentrations measured during July 1998, which provides new insight into the timescales related to cross-tropopause transport processes.

2. Aircraft Measurement Campaigns

[7] The NMHC measurements from canister samples, as well as the in situ data presented here, were obtained during three different STREAM campaigns carried out in the upper troposphere and lower stratosphere (LS) between 40° and 80°N. The measurement flights were performed with a twinjet Cessna Citation operated by the Delft University of Technology in Netherlands. The first campaign, STREAM 1995, took place during November and the beginning of December in 1995. Four flights were conducted from Amsterdam (Netherlands, 52°N, 4.5°E) during which 21 canister samples were collected representing the fall season between 52° and 55°N. Second, a late-winter
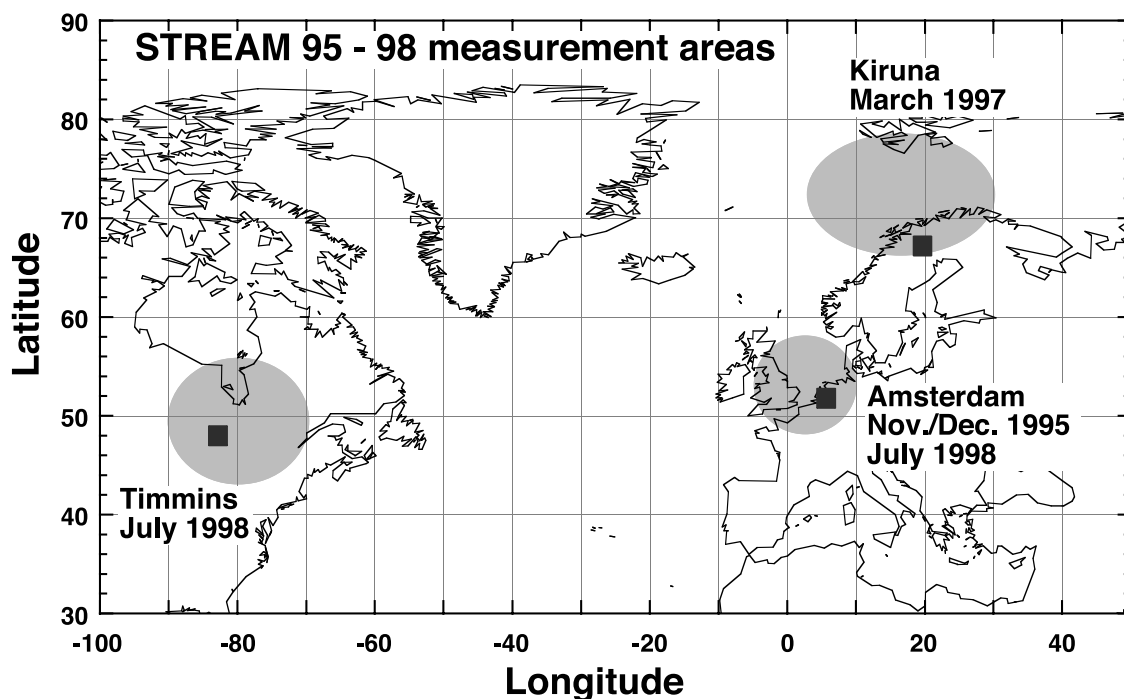
Figure 1. Overview of the measurement areas covered by the STREAM campaigns performed in 1995, 1997, and 1998. The squares denote the airport locations from where the flights were conducted.

campaign (STREAM 1997) took place from Kiruna (Sweden, 68°N, 20°E) during March 1997. Here 4 flights conducted between 68° and 78°N yielded 29 canister samples. Finally, during the summer campaign (STREAM 1998) eight flights were carried out from Timmins (Canada, 48.2°N, 70.3°W) within the 44°–56°N latitude band and two flights from Amsterdam (flown between 47° and 57°N). The STREAM 1998 campaign yielded 90 canister samples including those collected during the ferry flight from Timmins back to Amsterdam. An overview of the measurement areas covered by the different STREAM campaigns is given in Figure 1.

[8] The major objectives of the STREAM campaigns were (1) to investigate the chemical composition of the upper troposphere and lower stratosphere as a function of season and latitude, (2) to study the extent and role of cross-tropopause exchange processes on the chemical composition of the tropopause region, and (3) to identify the air mass origin (anthropogenic or natural, e.g., biomass burning) and the role of long-range transport therein. The flight duration was typically about 3.5–4 hours and consisted of several stacked flight legs up to 13 km altitude (~160 hPa). During most flights the aircraft was able to reach the lower stratosphere at the cyclonic side of the polar jet, north of the polar front. In Table 1 we summarize the approximate Θ range where the tropopause was located during the different campaigns. Clearly, the tropopause height during summer is located above the winter tropopause, whereas the (late) fall tropopause height marks a transition between both seasons.

[9] The highest isentropic levels up to Θ = 370 K in the lowermost stratosphere were reached by the aircraft during July 1998. On the anticyclonic side of the jet stream, however, the tropopause height was usually at or above the maximum flight altitude of the aircraft (~13 km).

Meteorological forecast and analysis products (e.g., back trajectories) from the European Center for Medium Range Weather Forecasts (ECMWF), provided by the Royal Netherlands Meteorological Institute (KNMI), were used for flight planning and postcampaign data analyses. For more details about the STREAM 1995–1997 campaigns as well as measurement results we refer to *Lelieveld et al.* [1999], *Bregman et al.* [2000], and *Fischer et al.* [2000], and for the STREAM 1998 campaign to *Fischer et al.* [2002], *Hoor et al.* [2002], and *Lange* [2001].

3. Measurement Techniques

[10] NMHC were detected in whole air samples. A semi-automated grab sampling system, developed at Utrecht University, was used to fill nine precleaned 2.4-L electro-polished stainless steel canisters per flight at ~2.5 bar overpressure. Air was drawn in through a backward-facing stainless steel inlet by means of a metal bellows pump (MB-602). The filling of a canister took up to 3 min at ambient pressures of 160 hPa. Canister samples were analyzed in the laboratory by a gas chromatograph (GC) equipped with flame ionization detection (FID) for NMHC and electron capture detection (ECD) for halocarbons in 1–2 L cryogenically preconcentrated air samples. For more details about the GC analysis equipment and methods applied during STREAM 1995–1997 we refer to *Lelieveld et al.* [1999], and to *Rudolph* [1999] and *Fischer et al.* [2002] for STREAM 1998, for which the analyses were done at York University (Toronto, Canada). Part of the GC analysis during STREAM 1998 (ferry flight back and last two flights 9 and 10) was done at Utrecht University for which we refer to *Scheeren et al.* [2002] for technical details. Here we report results for a selected

Table 1. Overview of the Θ Range Denoting the Local Tropopause During the Different Campaigns and the Θ Range Representing the Extent of the Measurement Flights

Campaign	Period	Latitude Range	Θ Range Tropopause, K	Θ Range of All Flights, K
STREAM 1995	November–December 1995	52°–55°N	310–340 K	305–360 K
STREAM 1997	March 1997	60°–78°N	290–320 K	260–360 K
STREAM 1998	July 1998	44°–56°N	320–360 K	290–370 K

group of C_2–C_6 NMHC, being ethane (C_2H_6), acetylene (C_2H_2), propane (C_3H_8), n-butane (n-C_4H_{10}), isobutane (iso-C_4H_{10}), n-pentane (n-C_5H_{12}), isopentane (iso-C_5H_{12}), benzene (C_6H_6)), and methyl chloride. Routine calibrations with commercial standard gas mixtures resulted in an accuracy better than 10% for the STREAM 1995–1997 results and an accuracy better than 5% for the STREAM 1998 results. For the STREAM 1995–1997 measurement, precisions ranged between 2 and 14%, whereas for the STREAM 1998 measurements precisions were between 2 and 5%, depending on the species for concentrations larger than 15 parts per trillion by volume (pptv) (pptv, 10^{-12} mol mol^{-1}). At concentrations ≤5 pptv the precision is ≥50%. By measuring within a few weeks after collecting the air-sample storage artifacts were minimized and stayed within the uncertainty of the measurements.

[11] Ozone was measured at 1-Hz resolution with a modified pressure-independent chemiluminescence BENDIX 8002 monitor with a 1σ precision of 2% [*Lelieveld et al.*, 1997]. The absolute accuracy of the measurement is about 5% based on titration with a NO-standard gas before and after the campaign.

[12] CO and N_2O were measured by Tunable Diode Laser Absorption Spectroscopy (TDLAS) with Tracer In situ TDLAS for Atmospheric Research (TRISTAR) instrument from the MPI Mainz at a 1-Hz resolution, described in detail by *Wienhold et al.* [1998]. Calibrations with secondary standard were performed in situ during flight resulting in a 1σ precision of ±3.5% for CO and N_2O. Absolute calibration was deduced from cross-calibration with a primary standard resulting in a calibration accuracy of ±2.8% for both compounds, yielding a total uncertainty of 4.5%.

[13] Additional measurements of N_2O, as well as the measurement of CFC-12, were obtained with the global horizontal sounding technique (GHOST) from Frankfurt University at a rate of one sample every 2 min [*Bujok et al.*, 2001]. A precision (2σ) of ±0.90 and ±1.20% and an accuracy based on in-flight calibrations of ±2.51 and ±2.39% were obtained for N_2O and CFC-12, respectively. A comparison between the TDLAS and GHOST N_2O measurements showed average deviations of less than ±1.5%, which is within the accuracy range of both measurements [*Hoor et al.*, 1999].

[14] The acetone measurements were performed using a chemical ionization mass spectrometer (CIMS) from the MPI Heidelberg [*Spreng and Arnold*, 1994]. Acetone is chemically ionized by the proton transfer with H_3O^+ ions, and the products are detected with a quadrupole mass spectrometer. The precision (1σ) of the acetone measurement is about 15%, whereas the accuracy of the derived acetone concentration is ±30%. Acetone measurements with the CIMS have been compared to GC measurements, which

resulted in an agreement within the uncertainty range of the measurements [*Wohlfrom et al.*, 1999].

4. NMHC and Acetone in the Lowermost Stratosphere

4.1. Seasonal Variability

[15] Previous work has dealt with the abundance and chemistry of NMHC [e.g., *Rudolph et al.*, 1981; *Singh et al.*, 1997, 2000; *Lelieveld et al.*, 1999] and acetone [*Arnold et al.*, 1997; *Bregman et al.*, 1997; *Singh et al.*, 1997, 2000; *Wohlfrom et al.*, 1999] in the midlatitude lower stratosphere, focusing on a particular season. However, to our knowledge, seasonal variations in the abundance of reactive organic species in the extratropical lowermost stratosphere have not yet been studied. *Hoor et al.* [2002] describe a strong seasonality of transport from the troposphere to the stratosphere in the extratropics on the basis of the CO-O_3 relationship from the STREAM 1997 and 1998 campaigns. They showed that recent tropospheric influence during winter (STREAM 1997) does not extend beyond Θ = 20 K above the local tropopause, whereas during summer (STREAM 1998) tropospheric influences were found up to a potential temperature interval of Θ = 40 K or more. Here we investigate if a similar seasonality is present in the abundance of reactive organic compounds in the lowermost stratosphere. We examined the depth of the mixing layer for NMHC and acetone in terms of $\Delta\Theta$ relative to the local tropopause. Therefore the potential temperature of the local tropopause had to be taken into account for each flight. Similar to *Hoor et al.* [2002], we defined the upper boundary potential temperature value of the local tropopause along the flight track by an ozone concentration of 120 ppbv (ppbv = 10^{-9} mol mol^{-1}) in combination with a potential vorticity (PV) of 3.5 PV units (1 PV unit = 10^{-6} K m^2 kg^{-1} s^{-1}) [*Hoerling et al.*, 1993] as threshold values. PV along the flight track was derived from ECMWF analyses. Potential temperature at the tropopause was determined from the profile measurements.

[16] Table 2 presents an overview of selected C_2–C_6 NMHC (ethane, acetylene, propane, n-butane, isobutane, n-pentane, isopentane, and benzene) and other trace gas measurements in the lowermost stratosphere from November/December STREAM 1995, March STREAM 1997, and July STREAM 1998. In addition, we show mean results for the upper troposphere (7.5–12 km altitude). Note that for STREAM 1997 upper tropospheric measurements were only available for 23 and 25 March. For a detailed analysis of NMHC mixing ratios in the upper troposphere during STREAM 1998 we refer to *Fischer et al.* [2002]. The results in Table 2 represent the mean and 1σ standard deviation of a number of measurements performed in the upper troposphere and lowermost stratosphere at $\Delta\Theta$ = 0–30 K and at

Table 2. Overview of Results From STREAM 1995, 1997, and 1998 Averaged Over the Upper Troposphere, the Lower Stratospheric $\Delta\Theta = 0-30$ K Mixing Layer, and the Stratosphere at $\Delta\Theta > 30$ K Relative to the Local Tropopause[a]

Species/Campaign	Nov.–Dec. 1995 Upper Troposphere Mean (N = 6)	Nov.–Dec. 1995 Lower Stratosphere $\Delta\Theta$ 0–30 K (N = 8)	Nov.–Dec. 1995 Lower Stratosphere $\Delta\Theta$ > 30 K (N = 3)	March 1997 Upper Troposphere Mean (N = 1)	March 1997 Lower Stratosphere $\Delta\Theta$ 0–30 K (N = 15)	March 1997 Lower Stratosphere $\Delta\Theta$ > 30 K (N = 12)	July 1998 Upper Troposphere Mean (N = 23)	July 1998 Lower Stratosphere $\Delta\Theta$ 0–30 K (N = 23)	July 1998 Lower Stratosphere $\Delta\Theta$ > 30 K (N = 15)
O_3, ppbv	61 ± 19	198 ± 55	318 ± 11	46 ± 8	287 ± 65	558 ± 64	69 ± 18	326 ± 84	419 ± 52
PV units	1.2 ± 0.9	5.9 ± 0.9	7.8 ± 0.3	~1	5.9 ± 1.3	8.4 ± 0.5	0.9 ± 0.8	8.1 ± 2.4	9.2 ± 0.6
Θ, K	312 ± 5	341 ± 12	351 ± 4	~300	331 ± 9	346 ± 5	333 ± 8	345 ± 8	364 ± 3
$\Delta\Theta$	-14 ± 10	16 ± 9	37 ± 7	-20	20 ± 8	41 ± 7	-10 ± 6	17 ± 9	38 ± 3
N_2O, ppbv	n.a.	n.a.	n.a.	309 ± 2	297 ± 4	282 ± 6	312 ± 2	293 ± 8	287 ± 5
CFC-12, pptv	531 ± 5	506 ± 15	483 ± 9	538 ± 3	505 ± 8	469 ± 13	540 ± 7	494 ± 13	480 ± 9
CO, ppbv	n.a.	n.a.	n.a.	139 ± 16	37 ± 9	20 ± 3	116 ± 23	35 ± 18	20 ± 7
Acetone, pptv	790 ± 146	385 ± 112	279 ± 95	315 ± 40	113 ± 42	52 ± 8	2000 ± 509	430 ± 331	203 ± 63
C_2H_6, pptv	1101 ± 213	413 ± 100	250 ± 54	n.a.	219 ± 76	73 ± 24	1040 ± 346	303 ± 209	144 ± 106
C_2H_2, pptv	140 ± 27	25 ± 11	13 ± 3	n.a.	18 ± 14	1 ± 3	125 ± 38	40 ± 32	11 ± 7
C_3H_8, pptv	292 ± 192	24 ± 13	8 ± 4	n.a.	13 ± 7	3 ± 3	210 ± 82	28 ± 27	9 ± 6
$n\text{-}C_4H_{10}$, pptv	95 ± 60	5 ± 3	3 ± 1	n.a.	1 ± 2	<1	35 ± 25	6 ± 4	4 ± 2
$i\text{-}C_4H_{10}$, pptv	41 ± 30	2 ± 2	2 ± 2	n.a.	<1	<1	21 ± 11	5 ± 2	3 ± 1
$n\text{-}C_5H_{10}$, pptv	14 ± 11	4 ± 2	2 ± 1	n.a.	1 ± 2	<1	9 ± 5	3 ± 1	3 ± 2
$i\text{-}C_5H_{10}$, pptv	19 ± 15	3 ± 3	1 ± 2	n.a.	<1	<1	9 ± 8	3 ± 2	1 ± 1
C_6H_6, pptv	34 ± 24	5 ± 4	6 ± 3	n.a.	<1	<1	40 ± 31	10 ± 13	6 ± 3
$\Sigma C_2\text{--}C_6$, ppbC	4.27 ± 1.50	1.03 ± 0.27	0.62 ± 0.11	~3.2	0.52 ± 0.20	0.16 ± 0.06	3.45 ± 1.13	0.89 ± 0.57	0.41 ± 0.21
$\Sigma C_2\text{--}C_6$ + acetone, ppbC	6.64 ± 1.80	2.19 ± 0.54	1.46 ± 0.36	~4.1	0.86 ± 0.32	0.31 ± 0.07	9.5 ± 2.7	2.32 ± 1.7	0.76 ± 0.15

[a]Note that the STREAM 1997 free tropospheric concentrations were based on the flights of March 23 and 25 only, while the total C_2–C_6 NMHC (+ acetone) estimate is based on one canister sample (March 25). STREAM 1995 upper tropospheric acetone data are only available for the flight of November 29. N denotes the number of canisters. The variability denotes the 1σ standard deviation of the mean and n.a. denotes not available.

$\Delta\Theta > 30$ K. The range of $\Delta\Theta = 0-30$ K denotes the average depth of the (summer and winter) stratospheric mixing layer in accordance with *Hoor et al.* [2002].

[17] The values for O_3, CO, CFC-12, N_2O, acetone, and meteorological parameters (Θ, and PV from the ECMWF analysis along the flight track) are averaged from time series (and 1σ standard deviations) corresponding with the duration of the canister sampling (~3 min). The N_2O measurement results from the GHOST instrument were combined with results from the TDLAS instrument. In addition, we included the sum of total carbon for the selected C_2–C_6 NMHC and C_2–C_6 NMHC + acetone in nmol mol^{-1} carbon (parts per billion of carbon (ppbC)), as a measure of available reactive organic carbon (ROC). The selected C_2–C_6 NMHC represents more than 95% of the total NMHC that was detected during STREAM 1998 (which included isoprene, 2-methylbutane, 2,2-dimethylpropane, cyclohexane, methyl-cyclopentane, *n*-hexane, 2-methylpentane, 3-methylpentane, 2,2-dimethylbutane, toluene, methylcyclohexane, *n*-heptane, ethyl-benzene, *o*-xylene, *p*-, *m*-xylene, *n*-octane, and *n*-nonane detected close to their detection limit of ~5 pptv). We have to note, however, that the ROC values in this study underestimate the total amount of reactive organic species present in the atmosphere, since they do not include other important organic species such as formaldehyde, methanol, and peroxyacetyl nitrate (PAN).

[18] The mean NMHC + acetone concentration in the mixing layer ($\Delta\Theta = 0-30$ K above the local tropopause) of 2.2 ± 0.5 ppbC (Table 2) measured during the fall season (November/December 1995) compares well with the 2.3 ± 1.7 ppbC found during summer (July 1998), and both are more than a factor of 2 higher than the 0.9 ± 0.3 ppbC measured during winter (March 1997). The variability in the

ROC mixing ratios during summer, however, was about three times as large as that during fall. The variability is strongly dependent on the lifetime and source strength of the compound at the measurement location [e.g., *Jobson et al.*, 1999]. Hence a higher variability from one location to another (as in the summertime versus the fall lowermost stratosphere) is related to differences in the source and sink strength. The high lowermost stratospheric ROC variability during summer appears not to be reflected in the upper troposphere ("source") ROC variability as presented in Table 2. In terms of sink strength, on the other hand, photolysis and OH production are most likely higher in the summertime lowermost stratosphere as compared to fall conditions due to a higher solar zenith angle, thus enhancing ROC variability. In addition, the higher variability during summer suggests a higher frequency of cross-tropopause mixing events, presumably from more intense isentropic exchange at the subtropical jet during summer. The role of cross-tropopause transport on the LS ROC variability will be discussed further in section 5.1.

[19] Another point to be considered here is how seasonal variations of NMHC and acetone concentrations in the UT contribute to the seasonality observed in the LS. NMHC accumulate in the winter troposphere because of much longer photochemical lifetimes than in summer. Acetone, on the other hand, tends to be higher in the extratropical summer due to strongly enhanced terrestrial vegetation emissions and hydrocarbon oxidation processes [*Jacob et al.*, 2002]. Indeed, this seasonality is clearly reflected in the observed upper tropospheric ROC concentrations presented in Table 2. This can at least partly explain the high acetone concentrations in the summer LS. When we, however, consider the ratio of total UT to LS NMHC concentrations

Table 3. Estimate of Chemical Lifetimes, τ, in the Lowermost Stratosphere Based on Reaction Rate Coefficients k_{OH} and k_{Cl} (cm^3 molecule^{-1} s^{-1}), For Reaction With OH and Cl Radicals, Respectively[a]

Species	k_{OH} (223 K)[b]	k_{Cl} (223 K)[b]	$h\nu$	τ
N_2O	n.a	n.a	n.a	122 ± 24[c] years
CFC-12 (CCl_2F_2)	$<7 \times 10^{-18}$	n.a.	n.a.	87 ± 17[c] years
CFC-11 (CCl_3F)	$<5 \times 10^{-18}$	n.a	n.a	45[b] years
CO	1.63×10^{-13}	n.a	n.a	95 days
Ethane	6.5×10^{-14}	5.1×10^{-11}	n.a	100 days
Acetylene	3.3×10^{-13}	6.4×10^{-11}	n.a	29 days
Propane	5.0×10^{-13}	1.4×10^{-10}	n.a	18 days
Benzene	1.0×10^{-12}	n.a	n.a	12 days
Acetone	9.5×10^{-14}	n.a	$\sim 1.0 \times 10^{-6}$	11 days
n-Butane	1.4×10^{-12}	1.4×10^{-10}	n.a	8 days
n-Pentane	1.6×10^{-12}	1.4×10^{-10}	n.a	7 days

[a]The chemical lifetime, τ, of a species is defined as $\{k_{OH} [OH] + k_{Cl} [Cl]\}^{-1}$, where [OH] and [Cl] are the daily mean concentrations in molecules per cubic centimeter. We took the following mean ambient conditions in the lower stratosphere of 223 K, 150 mbar, [OH]: 10^6 molecules cm^{-3}; [Cl]: 10^3 molecules cm^{-3}. n.a. denotes not available.
[b]*Atkinson et al.* [2002].
[c]*Volk et al.* [1997].

(in parts per billion of carbon) we find a ratio of 4:1 for July and of 6:1 for March, while the upper tropospheric concentration equals ~3 ppbC for both seasons. It appears that in spite of the shorter photochemical lifetimes of NMHC during July, the higher NMHC values in the lower stratosphere are in agreement with enhanced and more frequent troposphere-to-stratosphere exchange taking place during summer [*Hoor et al.*, 2002].

[20] The abundances and vertical distributions of ROC species in the lowermost stratosphere provide a first measure of the extent of troposphere-to-stratosphere mixing and the photochemical age of the mixed air masses in the lowermost stratosphere. Notably, not only the presence of significantly higher amounts of acetone but also of ethane, acetylene, propane, and benzene during the fall and summer period, as compared to the winter, points to mixing timescales on the order of days to weeks based on the photochemical lifetimes of these tracer species in the lowermost stratosphere during summer as summarized in Table 3.

[21] The STREAM 1997 measurement results for the lowermost stratospheric mixing layer (Table 2; $\Delta \Theta <$ 30 K) compare well with the Pacific Exploratory Mission (PEM) West B measurements [*Singh et al.*, 1997] obtained in the lowermost stratosphere over the western/central Pacific (37°–57°N) during February/March 1994. We obtain good agreement within the variability of the mean mixing ratios for O_3, 334 ± 97 ppbv/287 ± 65 ppbv (PEM West B/STREAM 1997); CO, 44 ± 9 ppbv/37 ± 9 ppbv; $\Sigma C_2 - C_3$, 209 ± 134 pptv/250 ± 97 pptv; and acetone 153 ± 74 pptv/113 ± 42 pptv. In addition, mean concentrations for the lowermost stratospheric mixing layer during STREAM 1995 (November/December) are in accord with mean concentrations in the lowermost stratosphere over the Atlantic during October and November 1997 reported for the Subsonic Assessment, Ozone and Nitrogen Oxide Experiment (SONEX) campaign [*Singh et al.*, 2000]. Here we find for O_3, 191 ± 82 ppbv/198 ± 55 ppbv (SONEX/STREAM

1995); $\Sigma C_2 - C_3$, 461 ± 230 pptv/462 ± 124 pptv; and acetone 336 ± 225 pptv/385 ± 112 pptv. The comparison between the STREAM and PEM West B and SONEX results is illustrated in Figure 2. The good agreement is indicative of the hemispheric-scale seasonality in cross-tropopause exchange intensity with relatively weak exchange during the Northern Hemispheric winter and enhanced cross-tropopause exchange during fall.

[22] To further investigate the distribution of NMHC and acetone in the lowermost stratosphere during different seasons we looked at the total NMHC (parts per billion of carbon), acetone (parts per billion by volume), and NMHC + acetone (parts per billion of carbon) as a function of ambient ozone, shown in Figure 3. *Fischer et al.* [2000] and *Hoor et al.* [2002] used correlations between CO and ozone to show that in the absence of mixing processes across the extra-tropical tropopause, typically occurring on timescales of weeks, the ozone and CO relationship would approximate an "L"-shape, representing the "background" stratospheric and upper tropospheric reservoirs. Irreversible cross-tropopause mixing will result in mixing lines connecting both reservoirs with the slope being a function of the initial tracer mixing ratios and the time since the mixing event took place. The linearity of the ozone to CO relationship in the mixing zone is an indication of the intensity and frequency of the mixing process [*Hoor et al.*, 2002] and the homogeneity of the background stratospheric and upper tropospheric reservoir tracer mixing ratios. A steep slope ($\Delta O_3/\Delta CO$) characterizes aged air masses descended from the overworld, in which no recent mixing with tropospheric air has taken place and the major fraction of the ROC tracers has decayed photochemically.

[23] Figure 3 shows that a similar relationship between ozone, NMHC (+ acetone), and acetone as for CO [*Fischer et al.*, 2000] is present in the lowermost stratosphere. If we consider the upper part of the March 1997 (winter) branch
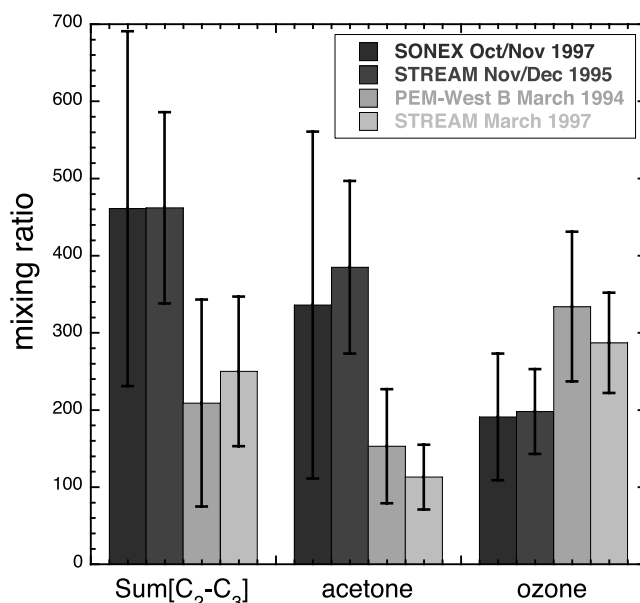
Figure 2. Comparison of results from STREAM 1995 and STREAM 1997 with the SONEX 1997 and PEM West B 1994 campaigns for the lowermost stratosphere. The error bars denote the measurement variability.
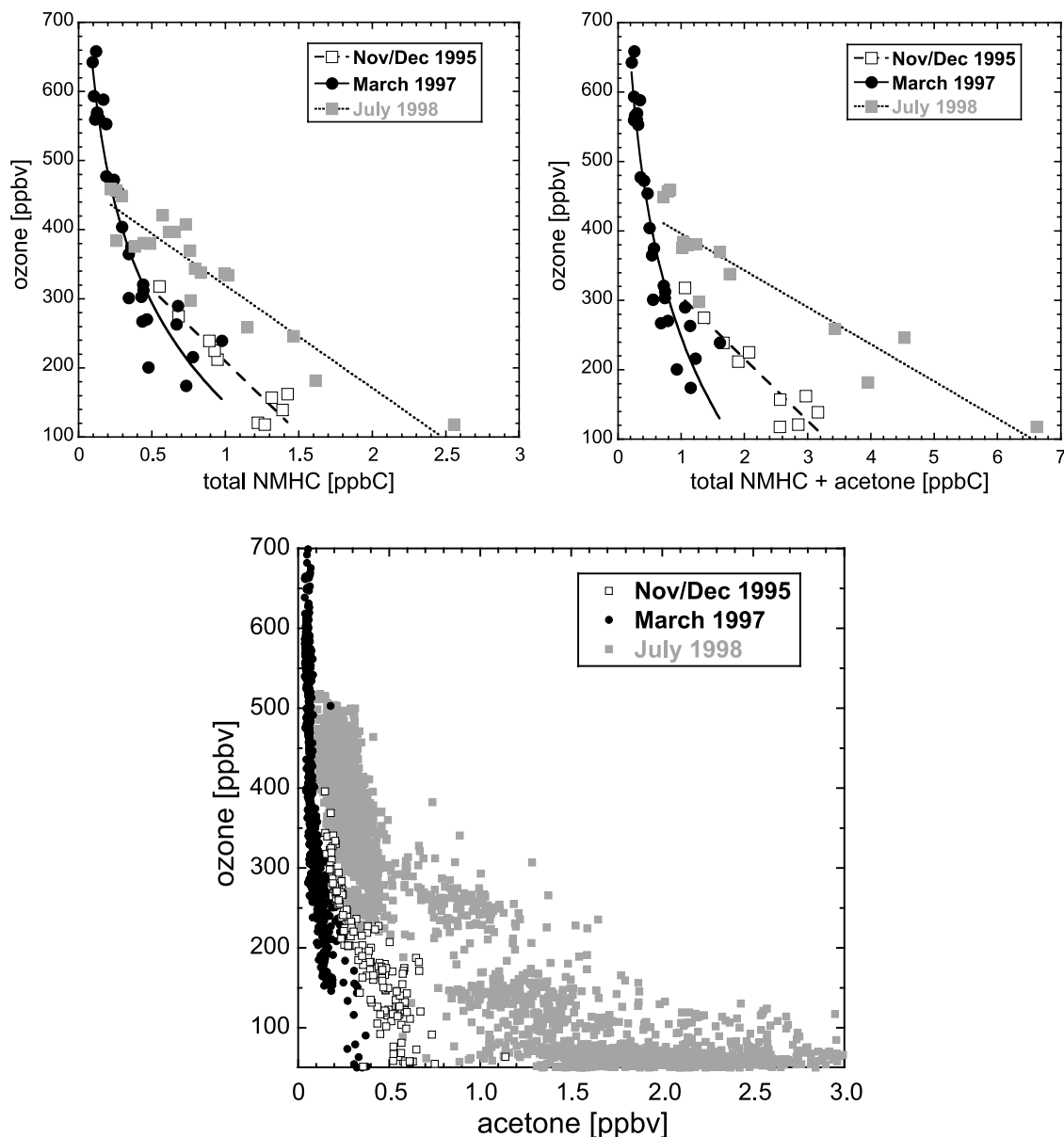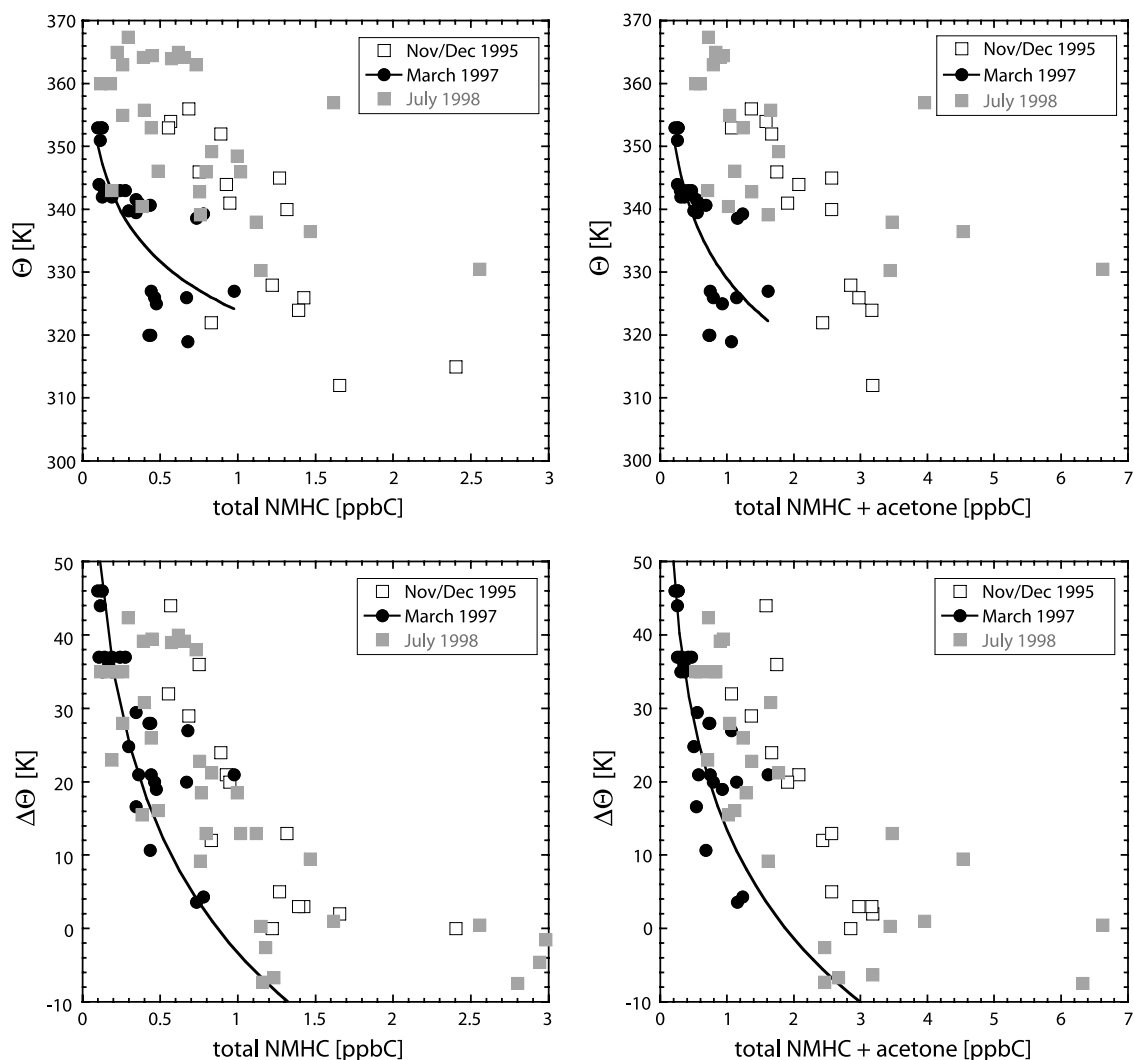
Figure 3. Total reactive NMHC in ppbC (first panel), NMHC + acetone in ppbC (second panel), and acetone in ppbv (third panel) and in ppbC as a function of the ozone concentration in the lower stratosphere for the March 1997, November/December 1995, and July 1998 campaigns. The third acetone panel includes acetone data in the upper troposphere for ozone concentrations between 50 and 100 ppbv. The curves represent the best fit through the data ($r = 0.9$), which is logarithmic for March 1997 and linear for November/December 1995 and July 1998. Precision error bars were left out for clarity (~5% for NMHC, 15% for acetone, and ~10% for NMHC + acetone).

of NMHC, representative of the "stratospheric reservoir," the November/December 1995 (fall) and July 1998 (summer) relationships resemble rather compact mixing lines ($r > 0.9$) in the lowermost stratosphere. The summer mixing line lies above the fall mixing line and extends to higher ozone concentrations, which indicates that mixing with tropospheric air extended deeper into the lowermost stratosphere, most likely as a result of intensified isentropic mass transport across the subtropical tropopause. The acetone-ozone relationship shows an identical seasonality as for NMHC, emphasizing its similar sources and sinks in the lowermost stratosphere. When acetone is included in the

total reactive carbon, the ppbC mixing ratio more than doubles, indicating its important role in the lower stratospheric ROC abundance. The relatively large variability of acetone in the lower stratosphere during July compared to the fall and winter season (Figure 3, third panel) appears to be related to high range in mixing ratios observed in the summertime upper troposphere. An additional probable cause is enhanced isentropic mixing at high potential temperatures in the summertime lower stratosphere.

[24] In Figure 4 the relationship between the potential temperature in the stratosphere and the amount of NMHC and NMHC + acetone (in ppbC) is presented for different

Figure 4. The relation between Θ in the stratosphere (first and second panels) and ΔΘ relative to the local tropopause (third and fourth panels), and the amount of reactive NMHC in ppbC (first and third panels) and NMHC + acetone (second and fourth panels) in the stratosphere for the different seasons. The logarithmic fit through the March 1997 data (winter) indicates the lower limit reference conditions when cross-tropopause transport at higher isentropic levels is reduced. Precision error bars were left out for clarity (∼5% for NMHC and ∼10% for NMHC + acetone).

seasons. To provide some qualitative information about the depth of the mixing layer we also included the vertical NMHC (and NMHC + acetone) distributions as a function of ΔΘ relative to the local tropopause. By using ΔΘ instead of Θ, the effect of varying tropopause heights is accounted for (as mentioned before, the upper boundary of tropopause is defined by the $O_3 = 120$ ppbv level and a PV of 3.5). The Θ-NMHC relationship in Figure 4 (first and second panels) clearly reveals that both the fall and summer NMHC (and NMHC + acetone) gradients lie above the winter gradient, extending to Θ levels of at least 370 K (the highest flight level). Furthermore, the fall and summer NMHC (and NMHC + acetone) gradients overlap, although it appears that the summer gradient extends deeper into the stratosphere (as function of Θ). However, if we correct for the local tropopause height and plot NMHC (and NMHC + acetone) as a function of ΔΘ (Figure 4, third and fourth

panels) we find an equally deep mixing layer for fall and summer extending to at least 40 K above the local tropopause. Note that during the fall season the tropopause was generally located at lower Θ levels than during summer, which partly explains the overlap.

[25]   From the ΔΘ-ppbC relationship in Figure 4 we can furthermore derive that during winter (March 1997) the amount of NMHC + acetone was 0.3 ± 0.1 ppbC at $\Delta\Theta > 30$ K above the local tropopause. We consider this as the lower stratospheric background, which is largely determined by acetone and ethane (∼50/50%). These background stratospheric acetone mixing ratios are in agreement with measurements by *Wohlfrom et al.* [1999], who report acetone mixing ratios of 100–200 pptv measured in the lower stratosphere over the North Atlantic during the Pollution from Air Traffic Emissions in the North Atlantic POLINAT-2/SONEX campaigns. During November/December 1995 and July 1998, on the other
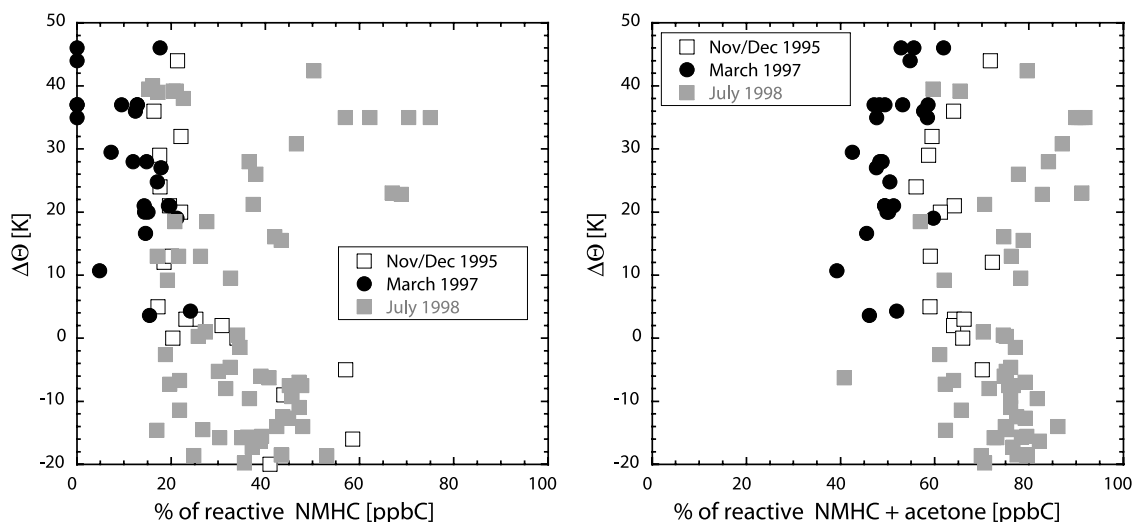
Figure 5. The relative fraction of reactive NMHC (minus ethane) and reactive NMHC (minus ethane) + acetone (in parts per billion of carbon) with chemical lifetimes between 1 and 4 weeks (Table 3; all C_3–C_6 NMHC + acetylene) as a function of $\Delta\Theta$ relative to the local tropopause. Precision error bars were left out for clarity.

hand, the amount of ROC (ppbC) was a factor of 3–5 higher at $\Delta\Theta > 30$ K as a result of intensified mixing with tropospheric air. This difference becomes even more significant by taking into account that the photochemical lifetimes of ROC species in the fall are relatively longer than in summer.

[26] Figure 5 shows the fraction of short-lived ROC species (in ppbC), which have chemical lifetimes between 1 and 4 weeks in the summertime lower stratosphere (see Table 3), relative to the total of ROC species as a function of $\Delta\Theta$. The vertical distribution clearly indicates that the fraction of short-lived ROC tracer species is strongly enhanced during summer, in spite of their shorter photochemical lifetime than in winter. While this fraction remains almost constant during the fall and winter conditions with increasing $\Delta\Theta$ (10–20% of NMHC; 40–60% of NMHC + acetone), a local maximum appears in the summer data between $\Delta\Theta = 20$ and 35 K (up to $\sim$70% for NMHC and $\sim$90% for NMHC + acetone). The highest fraction of "short-lived" ROC tracers was found around the 360 K isentrope ($\Delta\Theta = 30$), pointing to intensified mixing at the Θ levels during summer.

4.2. Role of Acetone

[27] As shown in the previous section, the amount of acetone (in ppbC) equals the sum of NMHC (in ppbC), hence it is the dominant organic tracer species in the lowermost stratosphere after ethane. Recently, *Jacob et al.* [2002] investigated the atmospheric budget of acetone with a 3-D model using extensive atmospheric observations. They found that the principal sources of acetone in the upper troposphere, notably in the tropics and Southern Hemisphere, are the terrestrial vegetation and the oceans. In the extratropical Northern Hemisphere winter, the oxidation of NMHC (notably propane, isobutane, and isopentane) dominates. This implies that acetone can be significantly enhanced over remote regions, such as the tropical Pacific, in the absence of significant anthropogenic

NMHC sources. *Dethof et al.* [2000] and *Hoor et al.* [2002] indicated that the summertime stratospheric mixing layer is subject to rapid and frequent mixing with tropospheric air. In fact, enhanced troposphere-to-stratosphere exchange at the subtropical jet over remote areas, where vegetation or oceanic sources of acetone dominate and NMHC concentrations are low, can explain the relatively high acetone concentrations in the lower stratosphere during summer.

[28] High acetone concentrations can lead to enhanced HO_x (HO_x = OH + HO_2) production from acetone photolysis in the presence of sufficient NO [*Singh et al.*, 1995], substantially enhancing the oxidizing capacity of the lowermost stratosphere during summer. HO_x formation from acetone photolysis begins with the production of methyl peroxy and acetyl peroxy radicals:

(R1) $CH_3COCH_3 + h\nu + 2O_2 \rightarrow CH_3O_2 + CH_3C(O)_2.$
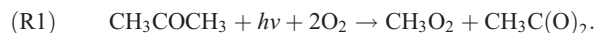
In the presence of sufficient NO most of the acetyl peroxy radicals are converted to methyl peroxy radicals forming HO_2 and NO_2 through reaction with NO. Subsequently, methyl peroxy reacts with NO and O_2 forming formaldehyde, HO_2, and again NO_2. The photolysis of NO_2 enhances ozone formation, which can be important in the background upper troposphere. Ultimately, the oxidation of an acetone molecule can lead to the production of $3.2HO_2$ radicals and $3O_3$ molecules [*Brühl et al.*, 2000].

[29] To investigate the impact of enhanced acetone concentrations on the HO_x budget we performed a box model study, which includes detailed acetone chemistry. For technical details of the box model setup we refer to *Brühl et al.* [2000]. Simulations were performed at the 225-hPa level, a mean temperature of 223 K, and chemical conditions in optimal agreement with observed mean conditions in the summertime lowermost stratospheric mixing layer during STREAM 1998. As such, CO and H_2O were kept fixed at 50 ppbv and 30 ppmv,
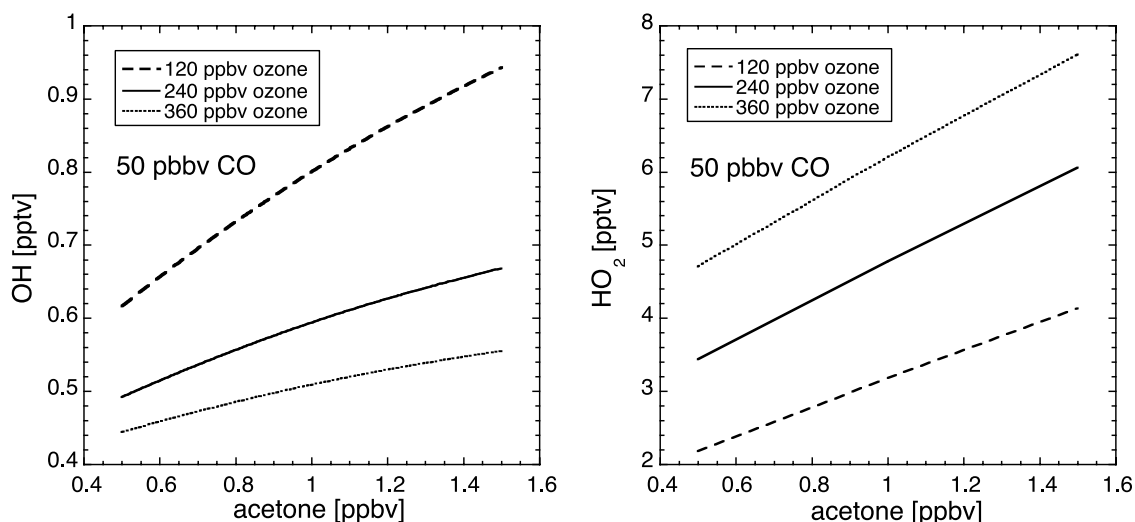
Figure 6. Box model noontime volume mixing ratios of OH and HO_2 as a function of acetone mixing ratios for the summertime lowermost stratosphere. Water vapor and CO have been fixed at 30 ppmv and 50 ppbv, respectively.

respectively. NO_x, HNO_3, and organic nitrates (mainly PAN) were initialized with 0.2, 2.0, and 0.45 ppbv, respectively, adding up to 2.65 ppbv, in good agreement with the mean observed total reactive nitrogen (NO_y) concentration of ~2.5 ± 1 ppbv in the stratospheric mixing layer during STREAM 1998 [*Lange*, 2001]. In Figure 6 we show simulations of noontime maximum OH concentrations ($[OH]_{max}$) as a function of acetone (ranging from 0.5 to 1.5 ppbv) for fixed ozone concentrations of 120, 240, and 360 ppbv. We find that the OH concentration is strongly dependent on available acetone. Under mean conditions of 240 ppbv O_3, the $[OH]_{max}$ ranges from 0.49 pptv at 0.5 ppbv acetone to 0.59 pptv at 1 ppbv acetone and 0.67 pptv at 1.5 ppbv acetone. This corresponds to diurnal mean OH concentrations for July conditions of 1.28, 1.54, and 1.74 $\times$ 10^6 molecules cm^{-3}, respectively. The $[OH]_{max}$ at background conditions of 20 ppbv of CO, 350 ppbv of ozone, and 250 pptv of acetone is 0.4 pptv, corresponding to a diurnal mean OH concentration of ~1 $\times$ 10^6 molecules cm^{-3}. This value is within the range of observed midday OH concentrations in the lowermost stratosphere of 0.2–0.5 pptv during the April/May 1996 SUCCESS mission [*Brune et al.*, 1998]. Summarizing, the observed acetone levels of 0.5–1 ppbv can explain 30–50% of the enhanced OH concentrations in the extratropical summertime lowermost stratosphere up to at least θ = 360 K. Finally, we note that recent laboratory work by *Blitz et al.* [2003] suggests that the present acetone photolysis rates, commonly used in chemical models, might be by a factor of 2 to those high. They indicate that the increase in HO_x production could be reduced by ~25% using their new photolysis rates.

4.3. Indications of (Sub)Tropical Air Mass Origin

[30] *Hoor et al.* [2002] used the CO-O_3 and CO_2-O_3 correlation to indicate that the elevated mixing layer, extending to at least Θ = 360 K in July (STREAM 1998), is caused by a stronger contribution of subtropical air mixed

into the lowermost stratosphere at the subtropical jet. Different anticorrelations appear as a result of mixing across the midlatitude and subtropical tropopause, respectively, due to the negative gradient of CO and positive gradient of CO_2 during summer toward lower latitudes [*Fischer et al.*, 2002]. We show in Figure 7 that the vertical profile of methyl chloride as a function of ozone provides additional evidence for mixing of low-latitude air into the lower stratosphere at potential temperatures of 360–370 K. It appears that the decreasing tendency of methyl chloride with increasing ozone reverses at about 450 ppbv, corresponding with a potential temperature of $\Delta\Theta \geq 30$ K. A probable explanation for enhanced methyl chloride at high potential temperatures ($\Theta > 360$ K) in the lower stratosphere could be transport across the tropical tropopause followed by fast horizontal mixing (<1 month) to midlatitudes first proposed by *Boering et al.* [1996]. Methyl chloride shows a global trend of increasing concentrations toward lower latitudes, throughout the tropical troposphere because its main emission sources such as oceans, biomass burning, and vegetation are strongest in the tropics [*Khalil et al.*, 1999; *Scheeren et al.*, 2002, 2003]. Consequently, higher CH_3Cl concentrations can be expected at higher isentropic levels (as was found during July 1998 (Figure 7)), for which the tropospheric influence from (sub)tropical regions is relatively strong.

5. Quantifying Troposphere-to-Stratosphere Transport

5.1. Fraction of Tropospheric Air in the Mixing Layer

[31] We described the summer lowermost stratosphere as a layer where air from the tropical and extratropical troposphere mixes with air descending from the stratospheric overworld. Since the mixing ratios of long-lived trace gases in the upper troposphere and stratospheric overworld are known (referred to as boundary conditions), along with the trace gas mixing ratio of these species in the mixing layer, the fraction of air from each of these source regions can be
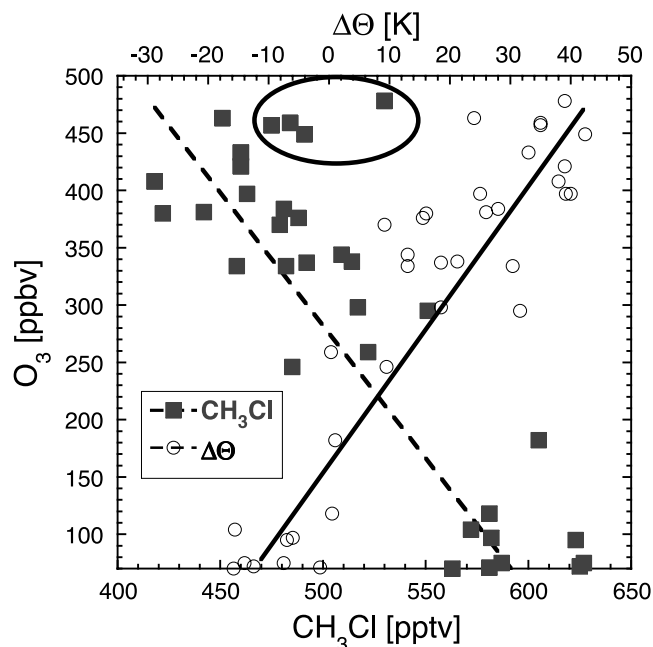
Figure 7. The vertical profile of methyl chloride and $\Delta\Theta$ as a function of O_3 for July 1998. The O_3-CH_3Cl relationship shows a decreasing tendency for CH_3Cl up to 450 ppbv of ozone (dashed line; $r = 0.83$). Above ~450 ppbv of O_3 we find enhanced CH_3Cl values relative to the trend (open circles). The solid line depicts the linear relationship between O_3 and $\Delta\Theta$ ($r = 0.93$). Precision error bars are left out for clarity ($O_3 \approx 5\%$, $CH_3Cl \approx 5\%$; $\Delta\Theta \approx 10\%$).

approximated by a simple mass balance equation analogous to *Ray et al.* [1999]:

$$\chi_{tse}(\Theta) = \chi_t(\Theta)N_t + \chi_s(1 - N_t), \qquad (1)$$

where $\chi_{tse}(\Theta)$ is the trace gas mixing ratio in the lowermost stratosphere as a function of potential temperature; $\chi_t(\Theta)$ is the upper tropospheric mixing ratio as a function of potential temperature and air mass origin; N_t is the fraction of tropospheric air in the lowermost stratosphere; and χ_s is the stratospheric overworld mixing ratio. A schematic representation of the composition of $\chi_{tse}(\Theta)$ is presented in Figure 8 showing the air-mass origins and transport pathways that determine the composition of the lowermost stratosphere.

[32] Rewriting equation (1) the fraction of tropospheric air, N_t, in the mixing layer can be described by

$$N_t = \{\chi_{tse}(\Theta) - \chi_s\}/\{\chi_t(\Theta) - \chi_s\}. \qquad (2)$$

The accuracy of N_t depends strongly on the accuracy and representativeness of the boundary conditions $\chi_t(\Theta)$ and χ_s. Furthermore, trace gases should have a significant difference in mixing ratios between the boundary conditions $\chi_t(\Theta)$ and χ_s in the upper troposphere and stratospheric overworld (larger than their variability). In this study, we used the long-lived tracers N_2O and CFC-12 (lifetimes of ~124 and ~87 years, respectively, see Table 3), which are

well mixed in the troposphere with nearly constant tropospheric concentrations over a 1-year period. In the stratosphere, however, these species have a strong gradient due to photochemical loss and vertical transport. In addition, we have used intermediately long-lived species such as CO and ethane, whose lifetimes of ~3 months far exceed that of reactive organic tracer species such as acetone, acetylene, propane, and benzene (10–40 days during summer over the continent; see Table 3) in the lowermost stratosphere. Both CO and ethane mixing ratios show a very strong gradient from the upper troposphere to the lower stratosphere, which is significantly larger than their observed variability (see Table 2).

[33] In Table 4 we present the boundary conditions, which have been derived from the measurement data for calculating N_t values. The N_t values have been calculated as the mean of the individual N_t, from hereon referred to as N_t^*, of N_2O, CFC-12, CO, and ethane when available, respectively. As such, the N_t^* values for the November/December 1995 campaign were based on CFC-12 and ethane only because measurement data for CO and N_2O were not available. For the March 1997 campaign upper tropospheric data for CO and C_2H_6 were considered too sparse to determine representative boundary conditions for these species. Here the N_t^* values were determined on the basis of N_2O and CFC-12 alone. The large data set for the July 1998 campaign allowed the determination of N_t^* on the basis of all selected long-lived tracer species. We found that using different tracer combinations has no significant effect
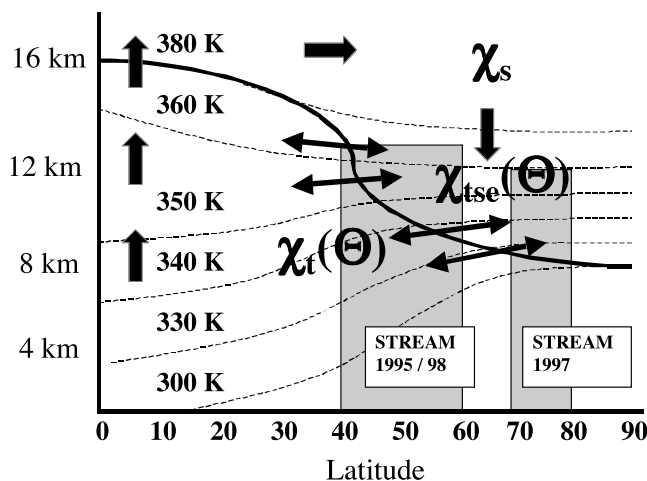
Figure 8. Schematic representation of the trace gas mixing ratio $\chi_{tse}(\Theta)$ in the lowermost stratosphere. The $\chi_{tse}(\Theta)$ mixing ratio is composed of air masses descending from above the 380-K surface with mixing ratio χ_s and tropospheric air masses with mixing ratio $\chi_t(\Theta)$. The solid line denotes the tropopause, whereas the thin dashed lines represent potential temperature isentropes. The shaded boxes mark the areas covered by the STREAM campaigns. Large-scale transport from the tropics to high latitudes (Brewer-Dobson circulation) is shown by single-headed arrows. Two-way exchange along isentropes associated with the subtropical and polar jet streams is shown as double-headed arrows. Upward transport across isentropes (diabatic ascent) can take place at midlatitudes (not shown).

Table 4. Overview of the Boundary Conditions as Used to Calculate the N_t Values for Different Campaigns[a]

Campaign	Boundary Conditions	N_2O, ppbv	CFC-12, pptv	CO, ppbv	C_2H_6, pptv
November/December 1995	upper troposphere	n.a.	531 ± 5	n.a.	1101 ± 213
	stratosphere	n.a.	464[b]	n.a.	40[c]
	$\theta \geq 360$ K				
March 1997	upper troposphere	309 ± 2	538 ± 3	n.a.	n.a.
	stratosphere	275 ± 4	458 ± 10	18 ± 2	54 ± 7
	$\theta \geq 353$ K				
July 1998	upper troposphere	312 ± 2	540 ± 7	116 ± 23	1040 ± 346
	stratosphere	283 ± 3	474 ± 5	15 ± 4	40 ± 20
	$\theta \geq 360$ K				

[a]The variability denotes the 1σ standard deviation of the mean. n.a. denotes not available.
[b]From interpolation to 360 K potential temperature.
[c]Adopted from STREAM 1998.

on the N_t^* estimates. N_t^* values for STREAM 1998, based on CFC-12 and ethane or on CFC-12 and N_2O alone, show an excellent 1:1 correlation ($r = 0.99$) with the N_t^* values based on all long-lived tracers.

[34] The accuracy of the mean N_t^* values is approximated by the variability (1σ standard deviation) of the long-lived tracer concentrations in the upper tropospheric and stratospheric reservoirs used to calculate N_t^* (see Tables 2 and 3). As such, a mean accuracy of ~10% for November/December 1995, ~1% for March 1997, and ~14% for July 1998 was determined. The precision, taken as the 1σ standard deviation of the mean of N_t^* values (based on the different long-lived species), was on average ~16% for November/December 1995, ~5% for March 1997, and ~6% for July 1998.

[35] In Figure 9 we show the calculated N_t^* values as a function of the total amount of ROC from NMHC and NMHC + acetone in ppbC in the upper troposphere and lower stratosphere for the different campaign seasons (precision error bars were left out for clarity). The data can be approximated by a logarithmic fit ($r = 0.95$) depicted in

Figure 9, although the stratospheric data at $N_t^* < 0.8$ show a rather linear relationship as well, in agreement with equation (2). Figure 9 further shows that during July 1998 (summer) the amount of NMHC was a factor of 2–3 higher than in March 1997 (winter) for a similar fraction of tropospheric air ($N_t^* < 80\%$) in the lowermost stratosphere. When we include acetone the difference is even a factor of 4–5. The results for the fall conditions (November/December 1995) appear to lie in between the winter and the summer case, being a transition between both annual extremes.

[36] In addition to the role of the upper tropospheric reservoir conditions (discussed in section 4.1), the seasonal difference in the stratospheric ppbC distributions as a function of N_t^* can also be interpreted in terms of differences in mean air-mass age. Closer to the tropopause, seasonal differences are smallest where cross-tropopause exchange can take place throughout the year, initiated by synoptic disturbances associated with the polar jet [*Chen*, 1995; *Dethof et al.*, 2000]. Thus depending on the mixing frequency, source strength, and photochemical age of the
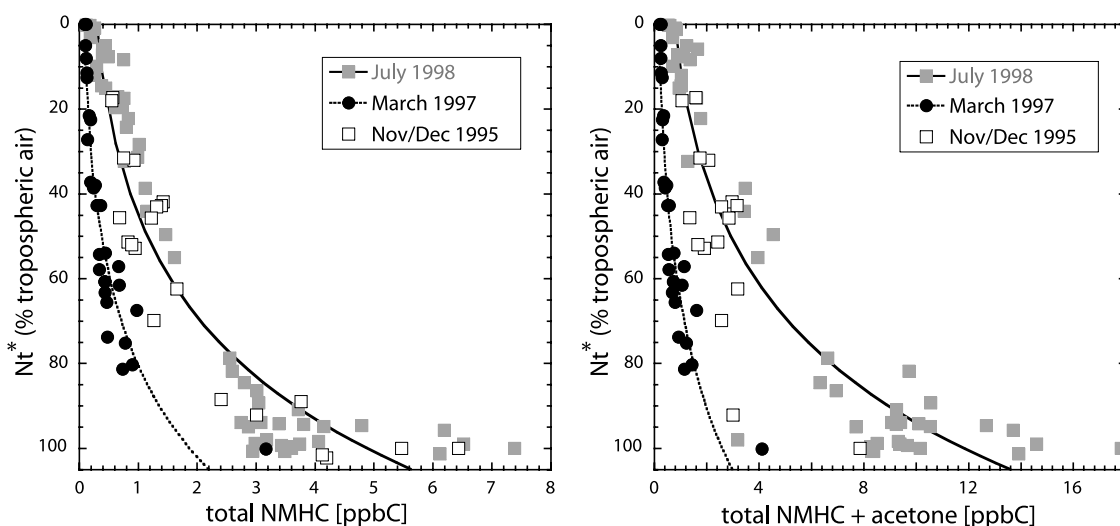
Figure 9. The total amount of measured reactive NMHC in ppbC as a function of the fraction of tropospheric air (N_t^*) in the upper troposphere and lower stratosphere for the different seasons. The curves represent the best fit (logarithmic; $r = 0.95$). Precision error bars are left out for clarity (~5% for NMHC and ~10% for NMHC + acetone; ~16% for N_t^*-1995, ~5% for N_t^*-1997, and ~6% for N_t^*-1998).
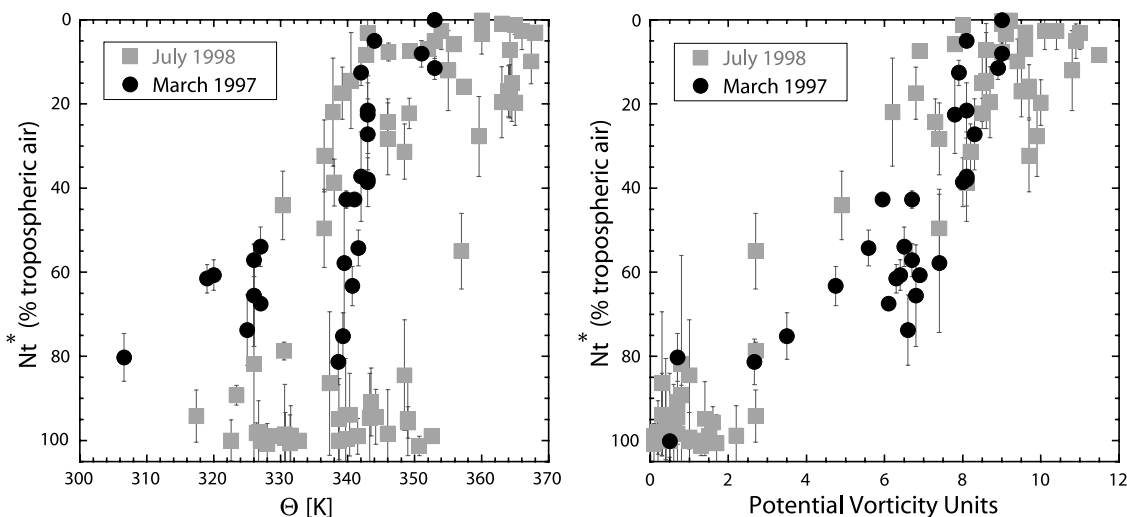
Figure 10. The fraction of tropospheric air (N_t^*) in the upper troposphere and lower stratosphere as a function of potential temperature (Θ) and potential vorticity is shown for March 1997 and July 1998. The data points correspond to the average conditions during canister sampling. The error bars denote the 1σ standard deviation of the mean N_t^* value (precision error bars of $\sim$10% for potential temperature and potential vorticity are left out for clarity).

organic species, their mixing ratios are maintained well above their background. Deeper in the mixing layer, at isentropic surfaces >340 K, the exchange frequency becomes seasonally dependent, and the fraction of aged stratospheric air increases. In addition, there is also a latitudinal effect to take into account. During summer, troposphere-to-stratosphere exchange (TSE) appears to be strongest at the subtropical tropopause. Tropospheric air masses mixed into the lowermost stratosphere that are transported poleward undergo chemical breakdown of reactive tracer species. Therefore air sampled at lower latitudes in the mixing layer can be less photochemically processed and can contain more reactive trace gases as compared to air masses sampled at higher latitudes with a similar tropospheric fraction.

[37] In Figure 10, the N_t^* in the upper troposphere and lower stratosphere as a function of potential temperature (Θ) and PV is shown for March 1997 and July 1998. Complementary to the results shown in Figure 9, Figure 10 (first panel) indicates that the tropospheric fraction, N_t^*, approaches zero at the $\Theta = 350$ K level during winter, whereas during summer mixing appears to extend to at least the $\Theta = 370$ K level. In agreement with this finding, the N_t^* as function of PV (Figure 10, second panel) emphasizes that enhanced ROC mixing ratios were found during winter up to about 9 PV units and up to at least $\sim$12 PV units during summer.

5.2. Transient Times of Tropospheric Air Masses

[38] Significantly enhanced NMHC mixing ratios of ethane, acetylene, and propane, as well as acetone, in the stratospheric mixing layer point to recent troposphere-to-stratosphere mixing events on timescales shorter than the estimated photochemical lifetimes of these species. A tropospheric filament in the lowermost stratosphere slowly dissipates by the photochemical decay of these reactive NMHC species and mixing with ambient air, while the long-lived species remain virtually unaffected. As a result,

the tropospheric fraction (N_t), determined from mixing ratios of the reactive NMHC species, becomes smaller than the tropospheric fraction calculated from the long-lived species (N_t^*) as a function of time (equation (2)). Since we know the boundary conditions $\chi_t(\Theta)$ and χ_s for the reactive organic species, their concentrations in the mixing layer $\chi_{tse}(\Theta)$ and the fraction of tropospheric air N_t^* (from long-lived species), we can estimate the time Δt a tropospheric air parcel spent in the stratospheric mixing layer from the moment the mixing event took place at t_0 and the encounter by the aircraft at t_1 ($\Delta t = t_1 - t_0$). Hence by introducing photochemical decay from the reactions with OH and Cl radicals into equation (1), we can describe the concentration of a reactive organic species in the mixing layer ($\chi_{tse}(\Theta)$) as follows:

$$\chi_{tse}(\Theta) = (N_t^*\{\chi_t(\Theta) - \chi_s\} + \chi_s)e^{-(k_{OH}[OH]+k_{Cl}[Cl])\Delta t}, \quad (3)$$

where k_{OH} is the rate coefficient for the reaction with OH; [OH] is the diurnal mean number density of OH in radicals cm^{-3}; k_{Cl} is the rate coefficient for the reaction with Cl; [Cl] is the daily mean number density of Cl in radicals cm^{-3}; and Δt is the transient time of the encountered air parcel in the lowermost stratosphere. From equation (3) we can write Δt as

$$\Delta t = \ln\{\chi_{tse}(\Theta)/(N_t^*\{\chi_t(\Theta) - \chi_s\} + \chi_s)\}/$$
$$- \{k_{OH}[OH] + k_{Cl}[Cl]\}. \quad (4)$$

The transient time Δt can be considered as the period between a discrete TSE event bringing tropospheric air masses into the lowermost stratosphere and the encounter with the measurement aircraft. As such, Δt provides a measure of typical timescales of mixing processes in the lowermost stratosphere. Clearly, only recent mixing events provide conditions with NMHC mixing ratios in the mixing layer well above the detection limit of $\sim$5 pptv. We chose
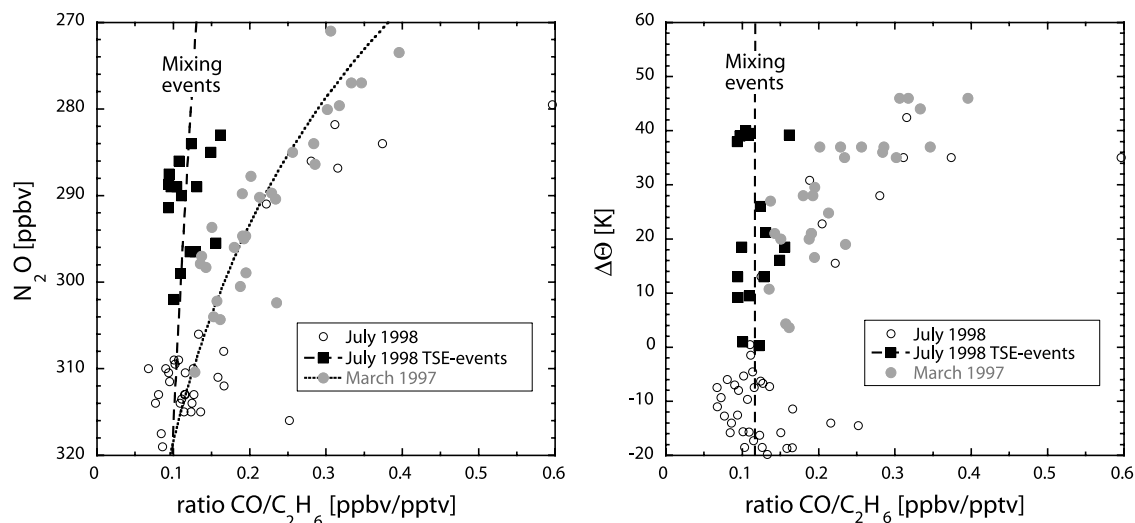
Figure 11. The ratio CO/C_2H_6 as a function of N_2O and $\Delta\Theta$ relative to the local tropopause. The STREAM 1997 "reference data" denote the March 1997 conditions with suppressed cross-tropopause transport (first panel exponential fit; $r = 0.9$). The recent STREAM 1998 TSE events stand out with a CO/C_2H_6 ratio closely related to values found in the upper troposphere (linear fit).

the 3σ precision of the stratospheric background concentration as lower limit excess value, considering mixing ratios ≥ 25 pptv as being significantly enhanced. In the following sections we apply the above transient time estimate method to a number of TSE events encountered during July 1998 over Canada and discuss the uncertainties involved.

5.3. Indications of Recent TSE Events

[39] The vertical distribution of the CO/C_2H_6 ratio appears to be a useful indicator of air masses with a strong tropospheric signature in the lowermost stratosphere due to a TSE event. Emissions of ethane and CO are highly correlated as a result of their common natural and anthropogenic sources [e.g., *Olivier et al.*, 1996]. Furthermore, the chemical lifetimes of both gases are of similar magnitude in the upper troposphere (~ 3 months) in the absence of a high (>1000) diurnal mean number density of Cl (in radicals cm^{-3}). As a result, the CO/C_2H_6 ratio is not very variable in the upper troposphere and appears to be not very dependent on location and season, as was shown earlier by *Lelieveld et al.* [1999]. They found a value of 0.11 ± 0.04 (ppbv pptv^{-1}) as arithmetic mean for the Northern Hemispheric upper troposphere from various measurements and campaigns. While the upper tropospheric concentrations of ethane and CO are typically around 1 and 100 ppbv, respectively (Table 2), concentrations in the background stratosphere are photochemically reduced to about 40 pptv or less of ethane and 15 ppbv of CO ($\theta > 360$ K; Table 3) resulting in a CO/C_2H_6 ratio ≥ 0.4. Because of this large concentration gradient, the CO/C_2H_6 ratio does not change significantly after mixing with stratosphere air depleted in C_2H_6 and CO for a certain period of time (lesser than the photochemical lifetime of ethane and CO). Eventually, the CO/C_2H_6 ratio slowly increases from further photochemical depletion of C_2H_6 due to reaction with Cl radicals and mixing with aged stratospheric air from aloft (with <40 pptv of C_2H_6). Thus an air mass with a CO/C_2H_6 ratio within the range of the upper tropospheric

mean points to a recent tropospheric origin. How recently this air mass has entered the lowermost stratosphere can be estimated from higher hydrocarbons like acetylene, propane, and *n*-butane (section 5.4). The CO/C_2H_6 ratio as a function of the N_2O mixing ratio and $\Delta\Theta$ above the local tropopause is plotted in Figure 11 showing the encountered mixing events (in total 18) as a separate linear branch. Note that Figure 11 includes only data from STREAM 1997 and 1998 due to missing CO data for STREAM 1995. Ratios within the 1σ variability of the tropospheric mean were detected up to N_2O values of 283 ppbv, which corresponded to the $\Theta = 370$ K isentropic level in the lowermost stratosphere during the July 1998 measurements.

5.4. Transient Times From Stream 1998 TSE Events

[40] We selected nine TSE events from the STREAM 1998 campaign for which the concentrations of acetylene and/or propane were sufficiently high (≥ 25 pptv) to calculate a transient time Δt (equation (4)). Acetone, although abundant enough, has not been included in this analysis because its variability in the upper troposphere is too large (2.5 ± 1.5 ppbv; see Figure 3, second panel), and possible acetone formation in the mixing layer from NMHC precursor species (mainly propane) cannot be excluded. The tropospheric fraction N_t^* has been calculated based on N_2O, CFC-12, CO, and ethane mixing ratios in the mixing layer (χ_{tse}) and boundary conditions for the upper troposphere ($\chi_t(\theta)$) and stratospheric overworld (χ_s). Reaction rate coefficients for reaction of acetylene and propane with OH and Cl radicals in the lower stratosphere were determined for mean ambient conditions of 223 K and 150 hPa (see Table 3). We used diurnal mean OH and Cl number densities of $[OH] = 1.3 \times 10^6$ molecules cm^{-3} and $[Cl] = 1000$ molecules cm^{-3} for the midlatitude summertime lowermost stratosphere, estimated with the photochemical box model (section 4.2). The selected TSE events, upper tropospheric and stratospheric boundary conditions, and the

Table 5. STREAM 1998 Boundary Conditions and Selected TSE Events[a]

Source Midlatitude/Polar	O_3, ppbv	PV, r.u.	Theta (Θ), K	$\Delta\Theta$, K	N_2O, ppbv	F-12, pptv	CO, ppbv	C_2H_6, pptv	C_2H_2, pptv	C_3H_8, pptv	N_t^*, %	$\Delta t\_C_2H_2$, days	$\Delta t\_C_3H_8$, days
Upper troposphere ($N = 23$)	69 ± 18	0.9 ± 0.8	333 ± 8	0	312 ± 2	540 ± 7	116 ± 23	1040 ± 346	125 ± 38	210 ± 82	0	n.a.	n.a.
Stratosphere ($N = 8$)	457 ± 15	9.3 ± 0.7	362 ± 4	>35	283 ± 2	474 ± 5	15 ± 4	40 ± 20	11 ± 5	10 ± 6	100	n.a.	n.a.
Mixing layer F1	338	8.5	349	21	289	492	34	260	48	31	22 ± 4	n.a.	8.5 ± 1.8
Mixing layer F2	246	7.4	337	10	299	513	54	493	76	60	50 ± 9	n.a.	9.0 ± 2.2
Mixing layer F4	259	4.9	330	1	296	510	52	427	50	35	44 ± 8	4.8 ± 0.9	15.6 ± 3.7
Mixing layer F5	n.a.	8.1	338	13	297	496	53	412	34	45	39 ± 5	11.4 ± 2.0	10.0 ± 2.2
Mixing layer F6	182	3.0	357	1	302	511	59	587	65	59	55 ± 9	2.9 ± 0.6	10.7 ± 2.6
Mixing layer F8	298	9.7	337	19	295	497	43	276	31	33	32 ± 8	10.3 ± 2.0	12.3 ± 2.9
Mixing layer ferry-a1	336	7.4	346	13	289	497	38	362	25	26	27 ± 8	12.3 ± 2.3	13.5 ± 3.2
Mixing layer ferry-a2	337	8.2	349	19	n.a.	497	39	393	31	29	31 ± 7	10.1 ± 1.9	13.8 ± 3.1
Mixing layer ferry-a3	408	8.7	363	38	291	483	27	283	29	20	20 ± 8	3.7 ± 0.7	n.a.

[a]The TSE events relate to measurements of C_2H_2 and C_3H_8 concentrations in the lowermost stratosphere, which are larger than the 3σ variability range of the stratospheric background conditions at $\Delta\Theta > 35$ K above the local tropopause. The variability denotes the measurement variability; except for N_t^*, $\Delta t\_C_2H_2$, and $\Delta t\_C_3H_8$, where the variability indicates the precision. r.u. stands for relative units. N denotes the number of canister samples. STREAM 1998 TSE events [OH]: 1.28×10^6 molecules cm^{-3}; [Cl]: 1000 molecules cm^{-3}. n.a. denotes not available.

calculated transient times based on acetylene ($\Delta t\_C_2H_2$) and propane ($\Delta t\_C_3H_8$) are presented in Table 5.

[41] The $\Delta\Theta$ values in Table 5 show that all but one (Ferry flight a3) of the selected TSE events occurred below the $\Delta\Theta = 25$ K isentropic surface. Hence with the assumption that isentropic transport of upper tropospheric air into the stratosphere below $\Delta\Theta = 25$ K took place in the region of the polar jet [*Hoor et al.*, 2002], we have used the mean of all data related to air masses with a midlatitude to high-latitude origin to define the upper tropospheric reservoir conditions shown in Table 5. *Fischer et al.* [2002], who investigated upper tropospheric tracer gradients during STREAM 1998, indicated that the highest concentrations of NMHC, which have strong anthropogenic sources (notably ethane, acetylene, propane), were detected in air masses of midlatitude to high-latitude origin. Lowest concentrations were found in air masses originating over the (sub)tropical Pacific with acetylene and propane mixing ratios as low as 40 and 20 pptv, respectively. Air mass origins in the upper troposphere, described in detail by *Fischer et al.* [2002], were based on 10-day backward trajectories (ECMWF). Although the CO/C_2H_6 ratio as a function of $\Delta\Theta$ (Figure 11) indicated in total seven more TSE events at $\Delta\Theta > 25$ K, the mixing ratios of acetylene and propane were mostly <25 pptv for these events and are therefore not included in Table 5. The low acetylene and propane mixing ratios above the $\Delta\Theta = 25$ K isentropic level suggest that these TSE events most likely took place over the (sub)tropical Pacific during July 1998.

[42] We find Δt values between 3 and 14 days in the mixing layer below $\Delta\Theta = 30$ K at a fraction of 20–60% of tropospheric air in the lowermost stratosphere during summer (Table 5). The variability of the Δt values denotes the estimated absolute precision. The precision is defined as the mean of the measured variability (1σ standard deviation of the mean) of the $\chi_t(\Theta)$ and χ_s mixing ratios and the 1σ standard deviation of the mean N_t^* value. The calculated fraction of tropospheric air for the mixing layer (July 1998) is in agreement with the range of 5–

55% estimated by *Hintsa et al.* [1998] from water vapor, CO_2, and O_3 aircraft measurements performed during May 1995. Our estimates for Δt support results from the model by *Dethof et al.* [2000]. They deduced that isentropic cross-tropopause exchange is a fast process occurring on a timescale of days. Furthermore, they found that the typical transition time for irreversible transport of a tropospheric filament into the lowermost stratosphere is 4–5 days.

5.5. Uncertainty of the Transient Time Estimates

[43] The results for $\Delta t\_C_2H_2$ and $\Delta t\_C_3H_8$ presented in Table 5 are not in perfect agreement. An important potential cause for erroneous results are wrongly defined tropospheric boundary conditions ($\chi_t(\Theta)$). A very low estimate of $\chi_t(\Theta)$ can result in an N_t value higher than the mean N_t^* value from stable tracers, which then results in a too low or even negative Δt value. The latter is the case for the first two examples of flight 1 (F1) and flight 2 (F2) in Table 5 for $\Delta t\_C_2H_2$ (written as n.a.). A very high estimate of $\chi_t(\Theta)$, on the other hand, will result in an overestimated Δt value. This might be the case for the difference in $\Delta t\_C_2H_2$ and $\Delta t\_C_3H_8$ for flights F4 and F6. The TSE events of F4 and F6 were encountered very close to the tropopause ($\Delta\Theta \approx 1$ K) and have a high tropospheric fraction ($N_t \approx 50\%$), pointing to a relatively recent mixing event in favor of the $\Delta t\_C_2H_2$ estimate. Furthermore, 10-day trajectories trace back to the midlatitude (F4) and (sub)tropical (F6) Pacific, where lower propane mixing ratios are expected. Hence by applying the lower range mixing ratio of 128 pptv for the propane tropospheric boundary condition for F4 and F6 we calculate a $\Delta t\_C_3H_8$ of 8.6 ± 2 and 3.6 ± 1 days, respectively, which is in much closer agreement with the $\Delta t\_C_2H_2$ values.

[44] Another uncertainty in the Δt estimate is the assumed [OH] and/or [Cl] radical number densities. It was shown earlier (section 4.2) that the acetone abundance strongly influences the OH concentration in the summertime lowermost stratosphere. The temperature dependence of the rate coefficients k_{OH} and k_{Cl} poses a potential
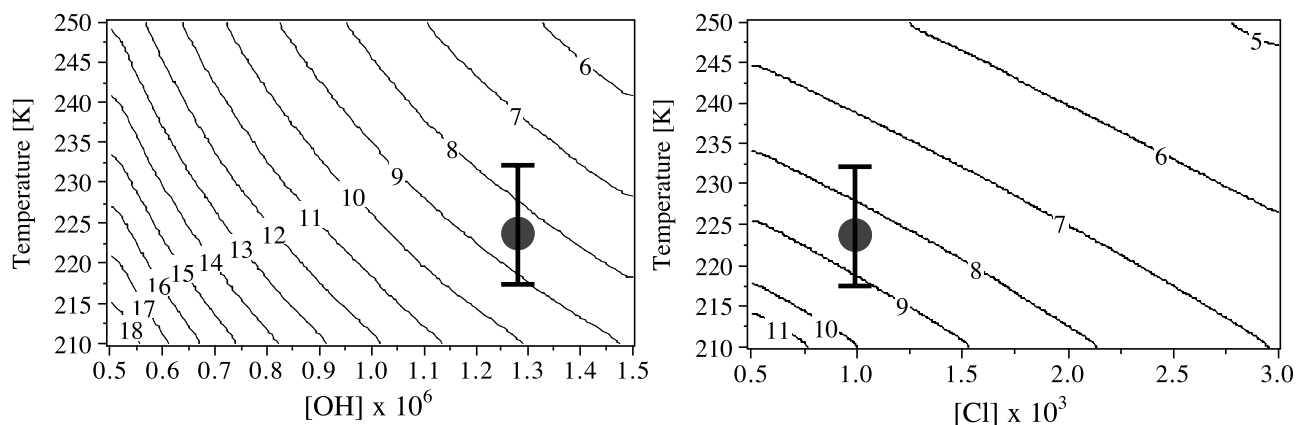
Figure 12.   Contour plots showing the sensitivity of the calculated residence time in days of the STREAM 1998 TSE event of flight 1 (F1 in Table 5) to ambient temperature and an increasing [OH] concentration (in 10^6 molecules cm^{-3}) in the first panel and to an increasing [Cl] concentration (in 10^3 molecules cm^{-3}) in the second panel. In the first panel the [Cl] concentration is fixed at 10^3 molecules cm^{-3}, whereas in the second panel the [OH] concentration is set at 1.3×10^6 molecules cm^{-3}. The shaded circle is the residence time calculated with the mean conditions chosen for the STREAM 1998 TSE events. The vertical bar denotes the ambient temperature range during the selected TSE events.

uncertainty as well. The sensitivity of the transient time estimates to ambient temperature, [OH], and [Cl] is depicted in Figure 12 using the selected mixing event of flight 1 (Table 5) as a starting point (gray dot). Both graphs indicate that an ambient temperature range of about ±10 K, encountered during the July 1998 flights (shown in the graphs by the vertical bar) causes an uncertainty in Δt on the order of a day (or an uncertainty of <10%). The calculated value for Δt is inversely proportional to the OH and Cl radical concentrations weighted according to the rate constants (equation (4)). Figure 12 shows that the Δt result could vary by ±2 days within the expected range of [OH] of ∼1− 1.5 molecules cm^{-3} as discussed in section 4.2. Varying the [Cl] concentration by a factor of 2 results in a variation of ±1.5 days.

6.   Conclusions

[45]   We presented data of selected $C_2 - C_6$ NMHC and acetone, which were collected during November/December 1995 (late fall), March 1997 (late winter), and July 1998 (summer) as part of STREAM in the extratropical lowermost stratosphere. The data augment the sparse reactive organic tracer measurements in the lowermost stratosphere. The NMHC and acetone measurements have been correlated with O_3, N_2O, and potential temperature revealing a strong seasonal variability in the abundance of reactive organic species in the extratropical lowermost stratosphere. We found enhanced concentrations of NMHC and acetone up to potential temperatures of 370 K during July 1998. During March, enhanced NMHC and acetone concentrations extended up to the $\Theta = 340$ K isentrope. The vertical distributions of MNHC and acetone follow the seasonal variations in mixing layer depth determined by *Hoor et al.* [2002] on the basis of correlations between CO and O_3. During summer and fall mean NMHC + acetone concentrations in the mixing layer equaled (2.3 ± 1.7 and 2.2 ± 0.5 ppbC, respectively) and were more than a factor of 2 higher than that measured during winter (0.9 ± 0.3 ppbC).

[46]   We note that the limited number of campaigns performed in different locations at different times requires caution in extrapolating our results to the whole lowermost stratosphere at all seasons and latitudes. Nevertheless, good agreement was found between mean results of STREAM (March 1997 and July 1998) and the February/March 1994 PEM West B campaign and the October/November 1997 SONEX campaign. In addition, our results cannot reveal possible effects from interannual variability in isentropic cross-tropopause transport on the organic tracer distributions in the lowermost stratosphere. Model work by *Dethof et al.* [2000] and M. Sprenger and H. Wernli (A Northern Hemispheric climatology of cross-tropopause exchange for the ERA15 time period (1979−1993), submitted to *Journal of Geophysical Research*, 2002) indicated, however, that the interannual variability of stratosphere-troposphere exchange is relatively small compared to its seasonal variability.

[47]   The amount of acetone (in parts per billion of carbon) equaled the sum of NMHC (in parts per billion of carbon) making it the dominant organic tracer species in the lowermost stratosphere after ethane. The relatively large acetone concentrations in the lowermost stratosphere as compared to NMHC, especially during summer, emphasize the dominance of terrestrial and oceanic sources in the upper troposphere as suggested by *Jacob et al.* [2002]. We used a box model to indicate that these acetone sources can explain 30− 50% of the enhanced OH concentrations in the summertime lowermost stratosphere up to at least $\Theta = 360$ K, through enhanced isentropic transport at the subtropical tropopause.

[48]   A simple mass balance calculation was used to estimate the transport of tropospheric air into the lowermost stratospheric mixing layer. It was found that a significant tropospheric fraction (≤30%) was present up to $\Theta = 370$ K during July 1998, while the tropospheric fraction during March 1997 approached zero at about $\Theta = 350$ K. Increasing methyl chloride concentrations at higher isentropic levels (360−370 K) in the lowermost stratosphere during July 1998 were found, pointing to a tropospheric fraction with a (sub)tropical origin.

[49] The decay of reactive organic species in the mixing layer with photochemical lifetimes of a few weeks during summer (notably propane and acetylene) was used to demonstrate a simple method based on a modified mass balance calculation to estimate timescales of troposphere-to-stratosphere mixing. A number of troposphere-to-stratosphere mixing events, encountered during July 1998, with acetylene and propane concentrations of $25-80$ pptv well above their detection limit could be used to calculate mixing timescales of $3-14$ days, indicating the transit time between the mixing event and the encounter with the aircraft. These results corroborate the studies of *Dethof et al.* [2000] and *Hoor et al.* [2002], demonstrating that the summertime midlatitude lowermost stratosphere is subject to intense and frequent mixing with tropospheric air. Our analysis of mixing timescales in the lowermost stratosphere during the 1998 summer is hampered, however, by the low number of encountered mixing events due to the limited canister sample frequency. By greatly increasing the number of NMHC measurements a better representation of the reservoir conditions could be achieved. At the same time, a larger number of TSE events will be encountered, allowing a more quantitative analysis.

References

Andrews, A. E., et al., Mean ages of stratospheric air derived from in situ observations of CO_2, CH_4, and N_2O, *J. Geophys. Res.*, *106*, 32,295–32,314, 2001.

Appenzeller, C., J. R. Holton, and K. H. Rosenhof, Seasonal variation of mass transport across the tropopause, *J. Geophys. Res.*, *101*, 15,071–15,078, 1996.

Arnold, F., V. Burger, B. Droste-Fanke, F. Grimm, A. Krieger, J. Schneider, and T. Stilp, Acetone in the upper troposphere and lower stratosphere: Impact on trace gases and aerosols, *Geophys. Res. Lett.*, *24*, 3017–3020, 1997.

Atkinson, R., D. L. Baulch, R. A. Cox, J. N. Crowley, R. F. Hampson Jr., J. A. Kerr, M. J. Rossi, and J. Troe, Summary of evaluated kinetic and photochemical data for atmospheric chemistry, IUPAC Subcomm. on Gas Kinetic Data Eval. for Atmos. Chem., Int. Union of Pure and Appl. Chem., Basal, Switzerland, 2002. (Available at http://www.iupac-kinetic.ch.cam.ac.uk/)

Bamber, D. J., P. G. W. Healey, B. M. R. Jones, S. A. Penkett, and G. Vaughan, Vertical profiles of tropospheric gases: Chemical consequences of stratospheric intrusions, *Atmos. Environ.*, *18*, 1759–1766, 1984.

Blitz, M. A., D. E. Heard, M. J. Pilling, S. R. Arnold, and M. P. Chipperfield, Implications for the UTLS HOx budget following a new measurement of the photodissociation quantum yields for acetone, paper presented at the EGS-AGU-EUG Joint Assembly, Nice, France, 6–11 April 2003.

Boering, K. A., B. C. Daube, S. C. Wofsy, M. Loewenstein, J. R. Podolske, and E. R. Keim, Tracer-tracer relationships and lower stratospheric dynamics: CO_2 and N_2O correlations during SPADE, *Geophys. Res. Lett.*, *21*, 2567–2570, 1994.

Boering, K. A., S. C. Wofsy, B. C. Daube, H. R. Schneider, M. Lowenstein, J. R. Podolske, and T. J. Conway, Stratospheric mean ages and transport rates from observations of carbon dioxide and nitrous oxide, *Science*, *274*, 1340–1343, 1996.

Bregman, A., et al., In situ trace gas and particle measurements in the summer lower stratosphere during STREAM II: Implications for O_3 production, *J. Atmos. Chem.*, *26*, 275–310, 1997.

Bregman, A., J. Lelieveld, M. van den Broek, P. Siegmund, H. Fischer, and O. Bujok, The N_2O and O_3 relationship in the lowermost stratosphere: A diagnostic for mixing processes as represented by a three-dimensional chemistry-transport model, *J. Geophys. Res.*, *105*, 17,279–17,290, 2000.

Brewer, A. W., Evidence for a world circulation provided by measurements of helium and water vapor in the stratosphere, *Q. J. R. Meteorol. Soc.*, *75*, 351–363, 1949.

Brühl, C., U. Pöschl, P. J. Crutzen, and B. Steil, Acetone and PAN in the upper troposphere: Impact on ozone production from aircraft emissions, *Atmos. Environ.*, *34*, 3931–3938, 2000.

Brune, W. H., et al., Airborne in-situ OH and HO_2 observations in the cloud-free troposphere and lower stratosphere during SUCCESS, *Geophys. Res. Lett.*, *25*, 1701–1704, 1998.

Bujok, O., et al., GHOST—A novel airborne gas chromatograph for in situ measurements of long-lived tracers in the lower stratosphere: Method and applications, *J. Atmos. Chem.*, *39*, 37–64, 2001.

Chen, P., Isentropic cross-tropopause mass exchange in the extratropics, *J. Geophys. Res.*, *100*, 16,661–16,673, 1995.

Dessler, A. E., E. J. Hintsa, E. M. Weinstock, J. G. Anderson, and K. R. Chan, Mechanism controlling the water vapor in the lower stratosphere: "A tale of two stratospheres," *J. Geophys. Res.*, *100*, 23,167–23,172, 1995.

Dethof, A., A. O'Neill, and J. Slingo, Quantification of the isentropic mass transport across the dynamical tropopause, *J. Geophys. Res.*, *105*, 12,279–12,293, 2000.

Fischer, H., F. G. Wienhold, P. Hoor, O. Bujok, C. Schiller, P. Siegmund, M. Ambaum, H. A. Scheeren, and J. Lelieveld, Tracer correlations in the northern high latitude lowermost stratosphere: Influence of cross-tropopause mass exchange, *Geophys. Res. Lett.*, *27*, 97–100, 2000.

Fischer, H., et al., Synoptic tracer gradients in the upper troposphere over central Canada during the STREAM 1998 summer campaign, *J. Geophys. Res.*, *107*, doi:10.1029/2000JD000312, 2002.

Fischer, H., et al., Deep convective injection of boundary layer air into the lowermost stratosphere at midlatitudes, *Atmos. Chem. Phys.*, *3*, 739–745, 2003.

Flocke, F., et al., An examination of chemistry and transport processes in the tropical lower stratosphere using observations of long-lived and short-lived compounds obtained during STRAT and POLARIS, *J. Geophys. Res.*, *104*, 26,625–26,642, 1999.

Hintsa, E. J., et al., Troposphere-to-stratosphere transport in the lowermost stratosphere from measurements of H_2O, CO_2, N_2O and O_3, *Geophys. Res. Lett.*, *25*, 2655–2658, 1998.

Hoerling, M. P., T. K. Schaack, and A. J. Lenzen, A global analysis of stratosphere-troposphere exchange during northern winter, *Mon. Weather Rev.*, *121*, 162–172, 1993.

Holton, J. R., P. H. Haynes, M. E. McIntyre, A. R. Douglass, R. B. Rood, and L. Pfister, Stratosphere-troposphere exchange, *Rev. Geophys.*, *33*, 403–439, 1995.

Hoor, P., H. Fischer, S. Wong, A. Engel, and T. Wetter, Intercomparison of airborne N_2O measurements using tunable diode laser absorption spectroscopy and in situ gas chromatography, *SPIE Proc.*, *3658*, 109–1115, 1999.

Hoor, P., H. Fischer, L. Lange, J. Lelieveld, and D. Brunner, Seasonal variation of a mixing layer in the tropopause region as identified by the CO-O_3 correlation from in-situ measurements, *J. Geophys. Res.*, *107*, doi:10.1029/2000JD000289, 2002.

Hoskins, B. J., Towards a PV-θ view of the general circulation, *Tellus, Ser. A*, *43*, 27–35, 1991.

Jacob, D. J., B. D. Field, E. M. Jin, I. Bey, Q. Li, J. A. Logan, and R. M. Yantosca, Atmospheric budget of acetone, *J. Geophys. Res.*, *107*, doi:10.1029/2001JD000694, 2002.

Jobson, B. T., S. A. McKeen, D. D. Parrish, F. C. Fehsenfeld, D. R. Blake, A. H. Goldstein, S. M. Schauffler, and J. W. Elkins, Trace gas mixing variability versus lifetime in the troposphere and stratosphere: Observations, *J. Geophys. Res.*, *104*, 16,090–16,113, 1999.

Khalil, M. A. K., R. M. Moore, D. B. Harper, J. M. Lobert, D. J. Erickson, V. Koropalov, W. T. Sturges, and W. C. Keene, Natural emissions of chlorine-containing gases: Reactive chlorine emission inventory, *J. Geophys. Res.*, *104*, 8333–8346, 1999.

Kritz, M. A., S. W. Rosner, E. F. Danielsen, and H. B. Selkirk, Air-mass origins and troposphere-to-stratosphere exchange associated with midlatitude cyclogenesis and tropopause folding inferred from ^{7}Be measurements, *J. Geophys. Res.*, *96*, 17,405–17,414, 1991.

Lacis, A. A., D. J. Weubbles, and J. A. Logan, Radiative forcing of climate by changes in the vertical distribution of ozone, *J. Geophys. Res.*, *95*, 9971–9981, 1990.

Lange, L., Aircraft-borne trace gas measurements during the STREAM 98 campaign, Ph.D. dissertation, pp. 71–93, Utrecht Univ., Utrecht, Netherlands, 2001.

Lelieveld, J., B. Bregman, F. Arnold, V. Bürger, P. J. Crutzen, H. Fischer, A. Waibel, P. Siegmund, and P. F. J. van Velthoven, Chemical perturbation of the lowermost stratosphere through exchange with the tropopause, *Geophys. Res. Lett.*, *24*, 603–606, 1997.

Lelieveld, J., A. Bregman, H. A. Scheeren, J. Ström, K. S. Carslaw, H. Fischer, P. C. Siegmund, and F. Arnold, Chlorine activation and ozone

destruction in the northern lowermost stratosphere, *J. Geophys. Res.*, *104*, 8201–8214, 1999.

Olivier, J. G. J., A. F. Bouwman, C. W. M. van der Maas, J. J. M. Berdowski, C. Veldt, J. P. J. Bloos, A. J. H. Visschendijk, P. Y. J. Zandveld, and J. L. Haverlag, Description of EDGAR version 2.0, *Rep. 771060 002*, Rijksinst. voor Volksgezondh. en Milieu, Bilthoven, Netherlands, 1996.

Poulida, O., R. Dickerson, and A. Heymsfield, Stratosphere-troposphere exchange in a midlatitude mesoscale convective complex, *J. Geophys. Res.*, *101*, 6823–6836, 1996.

Ray, E. A., F. L. Moore, J. W. Elkins, G. S. Dutton, D. W. Fahey, H. Vömel, S. J. Oltmans, and K. H. Rosenlof, Transport into the Northern Hemisphere lowermost stratosphere revealed by in situ tracer measurements, *J. Geophys. Res.*, *104*, 26,565–26,580, 1999.

Rood, R. B., A. R. Douglass, M. C. Cerniglia, and W. G. Read, Synoptic-scale mass exchange from the troposphere to the stratosphere, *J. Geophys. Res.*, *102*, 23,467–23,485, 1997.

Rudolph, J., Measurement of nonmethane hydrocarbons in the atmosphere, in *Volatile Organic Compounds in the Troposphere: Proceedings of the Workshop on Volatile Organic Compounds in the Troposphere, Jülich (Germany) October 27–31, 1997, Schriftenr. Forsch. Jülich*, vol. 16, edited by R. Koppmann and D. H. Ehhalt, pp. 11–35, Forsch. Jülich, Jülich, Germany, 1999.

Rudolph, J., D. H. Ehhalt, and A. Tönnissen, Vertical profiles of ethane and propane in the stratosphere, *J. Geophys. Res.*, *86*, 7267–7272, 1981.

Scheeren, H. A., J. Lelieveld, J. A. de Gouw, C. van der Veen, and H. Fischer, Methyl chloride and other chlorocarbons in polluted air during INDOEX, *J. Geophys. Res.*, *107*, doi:10.1029/2001JD001121, 2002.

Scheeren, H. A., J. Lelieveld, J. Williams, H. Fischer, and C. Warneke, Measurements of reactive chlorocarbons over the Surinam tropical rainforest: Indications for strong biogenic emissions, *Atmos. Chem. Phys. Discuss.*, *3*, 5469–5512, 2003.

Seo, K.-H., and K. P. Bowman, A climatology of cross-tropopause exchange, *J. Geophys. Res.*, *106*, 28,159–28,172, 2001.

Singh, H., et al., Distribution and fate of selected oxygenated organic species in the troposphere and lower stratosphere over the Atlantic, *J. Geophys. Res.*, *105*, 3795–3805, 2000.

Singh, H. B., M. Kanakidou, P. J. Crutzen, and D. J. Jacob, High concentrations and photochemical fate of oxygenated hydrocarbons in the global troposphere, *Nature*, *378*, 50–54, 1995.

Singh, H. B., Y. Chen, G. L. Gregory, G. W. Sachse, R. Talbot, D. R. Blake, Y. Kondo, J. D. Bradshaw, B. Heikes, and D. Thornton, Trace chemical measurements from the northern midlatitude lowermost stratosphere in early spring: Distributions, correlations, and fate, *Geophys. Res. Lett.*, *24*, 127–130, 1997.

Spreng, S., and F. Arnold, Balloon-borne mass spectrometer measurements of HNO_3 and HCN in the winter Arctic stratosphere—Evidence for HNO_3 processing by aerosols, *Geophys. Res. Lett.*, *21*, 1251–1254, 1994.

Vaughan, G., and C. Timmins, Transport of near-tropopause air into the lower midlatitude stratosphere, *Q. J. R. Meteorol. Soc.*, *124*, 1559–1578, 1998.

Volk, C. M., J. W. Elkins, D. W. Fahey, G. S. Dutton, J. M. Gilligan, M. Loewenstein, J. R. Podolske, K. R. Chan, and M. R. Gunson, On the evaluation of source gas lifetimes from stratospheric observations, *J. Geophys. Res.*, *102*, 25,543–25,564, 1997.

Wernli, H., and M. Bourqui, A Lagrangian "1-year climatology" of (deep) cross-tropopause exchange in the extratropical Northern Hemisphere, *J. Geophys. Res.*, *107*, doi:10.1029/2001JD000812, 2002.

Wienhold, F. G., et al., TRISTAR—A tracer in-situ TDLAS for atmospheric research, *Appl. Phys. B*, *67*, 411–417, 1998.

Wohlfrom, K.-H., T. Hauler, F. Arnold, and H. Singh, Acetone in the free troposphere and lower stratosphere: Aircraft-based CIMS and GC measurements over the North Atlantic and first comparison, *Geophys. Res. Lett.*, *26*, 2849–2852, 1999.

Zahn, A., Constraints on 20-way transport across the Arctic tropopause based on O_3 stratospheric tracer (SF_6) ages, and water vapor isotope (D, T) tracers, *J. Atmos. Chem.*, *39*, 303–325, 2001.

———————————

F. Arnold, Max Planck Institute for Nuclear Physics, Heidelberg, Germany.

B. Bregman, Royal Netherlands Meteorological Institute (KNMI), De Bilt, Netherlands.

C. Brühl, H. Fischer, and J. Lelieveld, Max Planck Institute for Chemistry, Mainz, Germany.

D. Brunner and P. Hoor, Institute for Atmospheric Science, Swiss Federal Institute of Technology, Zürich, Switzerland.

A. Engel, Institute for Meteorology and Geophysics, Johann Wolfgang Goethe University, Frankfurt, Germany.

J. Rudolph, Centre for Atmospheric Chemistry, York University, North York, Canada.

H. A. Scheeren and C. van der Veen, Institute for Marine and Atmospheric Research Utrecht (IMAU), Utrecht University, Physics and Astronomy, Princetonplein 5, P.O. Box 80005, Utrecht 3508 TA, Netherlands. (h.a.scheeren@phys.uu.nl)